NTNU – Trondheim
Norwegian University of
Science and Technology

Processing of Gustatory Information by Protocerebral Neurons in the Moth *Heliothis virescens*

Eirik Stamland Nilssen

Biology

Supervisor: Hanna Mustaparta, IBI
Co-supervisor: Pål Kvello, UC Berkeley
Bjarte Bye Løfaldli, IBI

Norwegian University of Science and Technology
Department of Biology

Acknowledgements

The work presented in this Master thesis was carried out at the Neuroscience unit, Department of Biology, Norwegian University of Science and Technology (NTNU) from August 2010 to June 2012, under the supervision of Professor Hanna Mustaparta, Doctor Pål Kvello and PhD student Bjarte Bye Løfaldli. The experimental and theoretical work conducted in this study have been of great interest and presented me with new and rewarding challenges.

First and foremost I would like to give special thanks to Pål Kvello. He has been of great assistance during the experimental work, as well as providing constructive feedback during the writing of the theisis. I am also grateful to Bjarte Bye Løfaldli for his enthusiasm, encouragement and for always answering my questions patiently. I especially want to thank my supervisor Hanna Mustaparta, who has been a great inspiration and motivation, and for helping me during the writing process. I am grateful to all of you for sharing your knowledge and for introducing me to the immensely fascinating field of neuroscience.

I would like to thank the other members of the Neuroscience unit, especially my fellow students, Siri, Bente and Øyvind, for great companionship during these two years.

Credit also goes to Jabir Ali Ouassou, who has helped out with the computational work and advised me in the statistical analyses, and Egbert Holtrop for proofreading the thesis.

Last, but not least, I want to thank my family for supporting and believing in me, and all my friends in Trondheim for making my time here exciting and memorable.

Trondheim, May 2012

Eirik S. Nilssen

Eirik Stamland Nilssen

Abstract

Insects are guided to potential host plants by visual and olfactory signals. Upon arrival they encounter various taste stimuli, ultimately deciding whether the plant is a proper food or oviposition source. The detection of gustatory stimuli by contact chemosensilla has been studied in several insect species, and intracellular recordings from neurons in the subesophageal ganglion (SOG) of *Heliothis virescens* have revealed responses to several taste qualities mediated by different appendages. However, how the information is further processed in higher gustatory areas and how it may lead to taste-related behavior is poorly understood. Important questions are where gustatory neurons (GNs) project in the protocerebrum and how they process information mediated by different appendages, i.e. the coding of taste identity and location. These topics were investigated in the present study using intracellular recordings combined with fluorescent staining techniques. The recordings were carried out *in vivo* from single neurons in the protocerebrum of the moth *Heliothis virescens*, while concurrently stimulating the contact chemosensilla of the antennae and the proboscis with gustatory and mechanosensory stimuli. The protocerebral neurons showed large diversity in their response tuning breadth, some responding specifically to one tastant applied at one appendage, whereas others responded to several tastants applied at one, two or three appendages. Some of the neurons were successfully stained, all of them partially or entirely located in the protocerebrum. In addition, some of the neurons targeted the SOG/tritocerebrum, the antennal mechanosensory and motor center (AMMC) and the antennal lobes (ALs). The present results point to different processing streams of taste information in the protocerebrum, where the narrowly tuned neurons seem to participate in a labelled line (LL) and the others in an across fiber pattern (AFP) mechanism. Moreover, the important role of the gustatory system for influencing behavior is substantiated by the widespread gustatory innervation of the protocerebrum. These projections suggest a role for the gustatory system in modulating the activity of other sensory systems, in addition to the coding of taste information.

Sammendrag

Smakssansen hos insekter er et essensielt redskap for å evaluere potensielle matkilder og eggleggingssteder. I flere studier hard et blitt satt fokus på det perifere smakssystemets oppbygning og funksjon. I tillegg er det vist at nevroner i det primære smakssenteret responderer på stimulering med flere smakskvaliteter på ulike appendiks. Hvordan smaksinformasjonen behandles i høyere smakssentre er derimot lite undersøkt. For å forstå dette bedre er det viktig å granske smaksnevronenes innerveringsmønster i protocerebrum og hvordan de responderer til stimulering med ulike smaksmodaliteter på flere appendiks. Disse spørsmålene har blitt undersøkt i denne studien ved bruk av intracellulære registreringer kombinert med fluoriserende fargeteknikker. De intracellulære registreringene ble utført fra enkeltnevroner lokalisert i protocerebrum av nattflyarten *Heliothis virescens*, samtidig som kontakt-kjemosensillene lokalisert på antennene og proboscis ble stimulert med mekanosensorisk stimuli og relevante smaksstimuli. De protocerebrale smaksnevronene varierte med hensyn til hvordan de responderte til stimulering med ulike modaliteter på forskjellige appendiks. Enkelte nevroner responderte spesifikt på stimulering med en modalitet på et appendiks, mens andre responderte på flere modaliteter på et eller flere appendiks. Noen av nevronene ble farget, og alle var helt eller delvis lokalisert i protocerebrum. I tillegg innerverte enkelte nevroner SOG/tritocerebrum, AMMC og antennelobene. Resultatene fra denne studien tyder på at smaksinformasjonen i protocerebrum behandles ved bruk av flere spatielle kodingsmekanismer; både populasjonskoding og "labelled line" koding ser ut til å operere i dette systemet. Videre er smakssansens betydning for dette insektet underbygget av smaksnevronenes omfattende innervering av protocerebrum.

Table of Contents

1 Introduction

The detection of chemical cues in the environment is of great importance to all organisms. In animals, the senses of taste (gustation) and smell (olfaction) reflect the sophisticated neural systems evolved for this task. The olfactory and gustatory systems, detecting volatile and dissolved compounds, respectively, are evolutionary old and serve many of the same functions in both vertebrates and invertebrates. The primary role of the gustatory system is to discriminate palatable, nutrient-rich compounds from compounds that are unpalatable and potentially harmful. Food sources rich in carbohydrates are perceived as pleasant by animals, leading to ingestion, whereas toxic compounds are usually unpleasant, leading to rejection. These behaviors are innate and essential for all animals when coping with the decision of whether to consume available food items. In insects, the sense of taste also contributes to the evaluation of potential places to deposit eggs (oviposition sites) (Schoonhoven, 1968; Ramaswamy *et al.*, 1987a; Thompson and Pellmyr, 1991; Renwick and Chew, 1994). The critical involvements of the gustatory system in regulating energy intake and reproduction have triggered scientists to look for the underlying neural mechanisms of insect gustation.

1.1 The organization of the peripheral gustatory system in insects

Insects have their taste organs located on several parts of the body, like the mouthparts, wings, tarsi, antennae and ovipositor (Dethier, 1955; Stocker, 1994; Amrein and Thorne, 2005). The chemosensory organs are named sensilla, consisting of an outer cuticle and a subcuticular matrix termed the sensillum lymph. In addition to housing neurons, the sensilla contain supporting non-neural cells responsible for establishing the appropriate ionic composition of the sensillum lymph (Dethier, 1955; Phillips and Vandeberg, 1976; Zacharuk and Shields, 1991). The sensilla are morphologically characterized and classified into several subtypes, like the *sensilla trichodea, sensilla chaetica, sensilla styloconica* and *sensilla placodea*. Among the different sensillum types, these four are identified to have gustatory function, but the same terms are also met for sensilla with olfactory (*s. trichodea* and *s. placodea*) and mechanosensory function (*s. trichodea*, *s. chaetica* and *s. styloconica)* (Schneider, 1964; Zacharuk and Shields, 1991). The gustatory sensilla contain the dendrites of several (usually three or four) gustatory receptor neurons (GRNs) and one mechanosensory dendrite, attached to the base. The dendrites of the GRNs extend to the distal end of the sensillum, where contact may be established with the external surroundings through an apical pore. In contrast to olfactory sensilla, gustatory sensilla must establish direct contact with an external surface in order to detect the stimuli. For that

reason, gustation is termed contact chemoreception and the gustatory sensilla are named contact chemosensilla (Larsen, 1962; Gaffal, 1979; Zacharuk, 1980; Hallberg, 1981).

1.2 Properties of GRNs

Insects are able to detect a large diversity of different substances, categorized into a few taste qualities. Their gustatory sensilla detect sugars, amino acids, salts, water, noxious compounds (equivalent to mammalian bitter compounds) and mechanosensory stimuli. In the blowfly *Phormia regina* and the fruit fly *Drosophila melanogaster*, a gustatory sensillum contains one mechano receptor neuron and four GRNs that are tuned to either salt, sugar, water or bitter compounds (Wolbarsht and Dethier, 1958; Dethier and Hanson, 1968; McCutchan, 1969; Dethier, 1977; Stocker, 1994; Liscia and Solari, 2000; Ozaki *et al.*, 2003; Amrein and Thorne, 2005). Electrophysiological recordings from the gustatory *s. chaetica* of the tobacco budworm moth *Heliothis virescens*e have revealed responses to bitter stimuli, sugars, amino acids, salts, water and alcohols (Jørgensen *et al.*, 2006; Jørgensen *et al.*, 2007a). In the honeybee *Apis mellifera*, responses to sugars and salts, but not to bitter compounds, have been recorded from GRNs located on the antennae (de Brito Sanchez *et al.*, 2005; de Brito Sanchez, 2011).

1.3 Gustatory receptors

A scan of the *D. melanogaster* genome uncovered a family of 60 genes suggested to encode gustatory receptors. The 60 genes encode 68 seven-transmembrane proteins, expressed almost exclusively in GRNs (Clyne *et al.*, 2000; Dunipace *et al.*, 2001; Scott *et al.*, 2001; Robertson *et al.*, 2003). Furthermore, multiple receptors are co-expressed in single GRNs (Wang *et al.*, 2004; Montell, 2009). The co-expression of Gr64f with either Gr5a or Gr64a is hypothesized to form a dimer, responsible for the detection of sugars (Jiao *et al.*, 2007; Jiao *et al.*, 2008; Isono and Morita, 2010). Similarly, bitter-tasting compounds are detected by a receptor complex, trimeric or multimeric in structure, in which Gr33a is an omnipresent subunit co-expressed with other gustatory receptors (e.g. Gr66a, Gr32a, Gr93a) (Thorne *et al.*, 2004; Lee *et al.*, 2009; Moon *et al.*, 2009; Isono and Morita, 2010). Four functionally different classes of bitter receptor neurons are identified, each class expressing a unique composition of bitter receptors (Weiss *et al.*, 2011). Importantly, receptors for sugars and bitter compounds are never co-expressed, proving the existence of non-overlapping populations of bitter and sugar receptor neurons (Scott, 2005). Receptors for salt and water do not seem to be present among any of the 60 gustatory receptor genes. In contrast, ion channels sensitive to changes in osmolarity are believed to be responsible for the transduction of water taste (Meunier *et al.*, 2009; Cameron *et al.*, 2010), whereas

amiloride-sensitive degenerin/epithelial sodium channels have been suggested as salt receptor candidates (Liu *et al.*, 2003). Less is known about the gustatory receptors in other insects, like *H. virescens* and *A. mellifera*. Currently, only one receptor, HR5, has been suggested as a candidate gustatory receptor in the tobacco budworm moth. This assumption is based on the expression of the receptor in sensory neurons associated with the *s. chaetica* located on the antennae (Krieger *et al.*, 2002). Ten gustatory receptor genes have been identified in the honeybee. Two of them encode receptors involved in sugar detection, whereas the remaining eight are not functionally characterized (Robertson and Wanner, 2006; de Brito Sanchez, 2011). Whether insect gustatory receptors signal by a metabotropic or ionotropic mechanism is presently a matter of debate (Bredendiek *et al.*, 2011; Sato *et al.*, 2011).

1.4 Projections of GRNs in the primary taste center

Unlike mammalian taste receptor cells, insect GRNs are primary bipolar neurons. GRNs located on the head, thorax and abdominal segments project their axons into corresponding ganglia in the central nervous system. GRNs located on the mouthparts and the antennae project their axons directly to the SOG/tritocerebrum, whereas GRNs on the wings and ovipositor project axons to thoracic or abdominal ganglia. Axons of GRNs located on some legs project to the SOG, whereas others project to thoracic or abdominal ganglia (Stocker, 1994; Singh, 1997; Mitchell *et al.*, 1999; Marella *et al.*, 2006). Because of the substantial gustatory innervation of the SOG, this ganglion is regarded as the insect primary taste center. It is formed by the merging of the mandibular, maxillary and labial neuromeres, and is fused with the tritocerebrum of the brain in some insects (Rehder, 1988; Mitchell *et al.*, 1999). In the SOG/tritocerebrum of *D. melanogaster*, axons of GRNs located on the internal mouthparts, the proboscis and the legs have been traced to spatially segregated areas (Stocker and Schorderet, 1981; Wang *et al.*, 2004). Similarly, axons of GRNs situated on the antennae and the proboscis in *H. virescens* project to close, but segregated areas of the dorsal SOG/tritocerebrum (Jørgensen *et al.*, 2006; Kvello *et al.*, 2006). In addition to this organotopic mapping, spatial mapping exists based on receptor neuron type, evident from the non-overlapping axonal projections of mechano receptor neurons and GRNs in the SOG/tritocerebrum of two mosquito species (Ignell and Hansson, 2005), the blowfly (Edgecomb and Murdock, 1992), the American cockroach (Nishino *et al.*, 2005) and the honeybee (de Brito Sanchez, 2011). In *H. virescens*, axon terminals of mechanosensory and gustatory receptor neurons have been found to be both segregated and partially overlapping. No segregation has been found for the axon terminals of GRNs projecting from one sensillum, suggesting that information about different gustatory modalities is relayed to the same area

(Jørgensen *et al.*, 2006). In contrast, in the SOG of the fruit fly, axons of GRNs detecting bitter stimuli terminate in a non-overlapping area from those detecting sugars, thus pointing to the existence of a taste quality map in this species (Wang *et al.*, 2004; Miyazaki and Ito, 2010).

1.5 Coding of gustatory information

Based on the tuning of GRNs to single taste qualities and their systematic projection pattern in the SOG, it is argued that encoding of gustatory information in the periphery follows an LL mechanism (Marella *et al.*, 2006). This means that information about a taste quality is encoded by narrowly tuned GNs, i.e. neurons tuned to one particular taste modality. The information is further relayed up the gustatory neuraxis following an independent pathway, segregated from pathways encoding other taste qualities (Hettinger and Frank, 1992; Erickson, 2000; Erickson, 2008). Thus, the information transfer is hardwired from the periphery to central targets. This organization implies that activation of a pathway is enough to provide information about the stimulus identity, whereas stimulus concentration is presumably mediated by the neuronal firing rate (Carleton *et al.*, 2010). Consistent with LL coding, intracellular recordings from the flesh fly *Sarcophaga bullata* provided evidence that SOG interneurons respond selectively to sucrose/water or salt. Some neurons responded to all three tastants and were considered purely mechanosensory (Mitchell and Itagaki, 1992). An equivalent study in *H. virescens* demonstrated that a large number of GNs in the SOG respond to different taste qualities applied at several appendages. Consequently, in this species, the activity of individual SOG neurons does not unequivocally state the specific taste quality or its application site, disagreeing with an LL scheme. Rather than engaging in an LL organization, the GNs seem to participate in a population code, more in accordance with an AFP model (Kvello *et al.*, 2010). In the context of gustation, the AFP model states the presence of a population of GNs that are broadly tuned, responding to stimulation with a broader range of taste modalities. The neurons respond with varying sensitivity to stimulation with different taste qualities, leading to the hypothesis that the combined activity of several neurons is necessary to code taste quality (Pfaffmann, 1959). Thus, the hallmark of the AFP model is that the message conveyed to postsynaptic neurons is present in the unique activity pattern of the neuronal ensemble (Hettinger and Frank, 1992; Erickson, 2000; Erickson, 2008).

1.6 Topics addressed in the present study

Progress has been made to understand the processing of gustatory information in the periphery and the first relay stations in the SOG and thoracic ganglia in insects. However, research on how gustatory information is processed in higher brain centers has been lagging behind. Results from a previous study of the SOG showed gustatory neurons projecting to the protocerebrum, indicating that gustatory processing occurs in this ganglion as well (Kvello *et al.*, 2010). This observation raised questions about the prevalence of GNs in the protocerebrum and how they handle gustatory information. By examining how the neurons respond to different modalities applied to different appendages, information is obtained regarding how this insect codes different gustatory stimuli. Furthermore, the morphology of the neurons will inform about where they receive and transmit information, and give indications to how they may be wired together in the gustatory neural network. These topics were explored in the present study. Intracellular recordings from single GNs in the protocerebrum of the moth *H. virescens* were carried out, during which the insect appendages were stimulated with mechanosensory and biologically relevant taste stimuli. The intracellular recordings were combined with fluorescent staining techniques, allowing visualization of the neurons. These methods enabled studying the following question:

- Which areas of the protocerebrum are innervated by protocerebral GNs?

Furthermore, neurophysiological analyses of the spike trains were carried out in order to inspect the following two hypotheses:

1. Protocerebral GNs respond to stimulation of several taste qualities applied at several appendages, i.e. they are broadly tuned with respect to stimulus identity and application site.
2. Broadly tuned protocerebral GNs participate in a discriminatory process of gustatory stimuli, by displaying differences in response strengths and temporal patterns to stimulation with different modalities.

2 Materials and Methods

2.1 The insects

The insects (*Heliothis virescens*; Heliothinae; Lepidoptera; Noctuidae) were acquired as pupae from a Swiss laboratory facility (Syngenta, Basel, Switzerland). Upon arrival, the pupae were sorted according to sex. After emerging as adults, the moths were transferred to cylindrical plexiglass containers (marked with the date of hatching) with perforated lids and supplied with a 5 % sucrose solution upon which they could feed *ad lib*. A maximum of eight animals were housed together in one container. The males and females were held in separate climate cabinets (Refritherm 200, Struers-Kebolab, Albertslund, Denmark, 22 °C) on a reversed LD photoperiod.

2.2 Preparation for electrophysiological recordings

On the day of the experiment, female moths (three to six days old) were selected and put in plastic tubes. Dental wax (Kerr Corporation, Romulus, MI, USA) was applied to fasten and immobilize the insect, exposing only the head. Tungsten clamps were utilized to keep the antennae and the proboscis in a fixed position, assuring that the contact chemosensilla would be exposed to stimulation throughout the experiment. Cephalic scales and hair present on the dorsal cuticle of the head were removed with a forceps, after which a microknife and a microscissor were used to remove the cuticle posterior to the antennae. Intracranial muscles and trachea were removed with a forceps to gain access to the left brain hemisphere, where the intracellular recordings were to take place. Ringer solution (in mM: 150 NaCl, 3 $CaCl_2$, 3 KCl, 25 $C_{12}H_{22}O_{11}$, 10 TES buffer; pH 6.9) was continuously administered to prevent dehydration of the brain tissue.

2.3 Intracellular recordings of protocerebral GNs

The plastic tube containing the moth was mounted in a holder and positioned under the microscope in the electrophysiological setup. The setup was situated inside a Faraday cage in order to block out external interference. A reference electrode (silver chloride coated silver wire) was inserted into the right compound eye. Neuronal activity was recorded using a sharp microelectrode of borosilicate glass, pulled with a flaming brown micropipette puller (P-97, Sutter Instrument Co., Novato, CA, USA). The resistance of the electrode was in the range 100-400 MΩ. The tip of the glass electrode was filled with the fluorescent dye tetramethylrhodamine-biotin dextran (Micro-Ruby; Invitrogen, Germany; 4%) and the electrode was backfilled with an electrolyte solution (0.2 M potassium acetate). A silver chloride coated

silver wire connected to a preamplifier (Axonprobe-1A, multipurpose microelectrode amplifier, Molecular Devices, CA, USA) was inserted into the fluid-filled microelectrode. The neuronal activity was visualized on an oscilloscope screen and the signal was digitalized through the use of the data acquisition unit CED (Micro 1401-03, Cambridge Electronic Design, Cambridge, England). The spike recording software Spike2 (v.7, CED), running a custom-made stimulation script, was used to record the neuronal activity. The recording electrode was inserted into the brain tissue with the use of a micromanipulator, and the insertion site was most frequently in the dorso-lateral area of the brain (the lateral protocerebrum). Some recordings were also carried out in the dorso-medial protocerebrum.

The stimuli used in the experiments were biologically relevant tastants (all from Merck Chemicals, Darmstadt, Germany; 1.0 M sucrose, 0.01 M quinine hydrochloride, 0.1 M NaCl), previously shown to activate the GRNs of the contact chemosensilla located on the antennae (Jørgensen *et al.*, 2007a), proboscis (Kvello, unpublished data) and tarsi (Boschker, 2010) in *H. virescens*. Tactile stimulation was also performed. All chemicals were dissolved in distilled water. The gustatory stimuli were applied as droplets on a glass rod to each appendage in the following sequence: left antenna, proboscis, right antenna. To each appendage the stimulation order was: sucrose, quinine, NaCl, tactile touch. If a stimulus evoked a response, the stimulation was repeated.

2.4 Staining of protocerebral GNs

GNs were stained by passing a 0.5-3 nA depolarizing current (pulses of 2 Hz, 0.2 s duration) through the recording electrode. The staining operation persisted as long as contact with the neuron was intact, usually between 5-15 minutes. Only a single staining procedure was performed in each brain preparation. After staining, the fluorescent dye was allowed to diffuse through the neuron over night at 4 °C. The following day, the brains were dissected in Ringer solution and fixed in paraformaldehyde (4 %) at 4 °C (24 hours) to prevent degradation of the neural tissue. The brains were treated with phosphate buffered saline (PBS; in mM: 684 NaCl, 13 KCl, 50.7 Na_2HP0_4, 5 KH_2PO_4; pH 7.2; 10 min) to wash out any remains of the fixative agent. To amplify the neuronal staining, the brains were immersed in Streptavidin-CY3 (Jackson Immunoresearch, West Grove, PA, USA) diluted in PBS (1: 200) at 4°C (24 hours), and subsequently rinsed in PBS (10 min). The preparations were dehydrated in an increasing ethanol sequence (50, 70, 90, 96, 100 %, 10 min each) to prepare for treatment in methyl 2-hydroxybenzoate (methyl salicylate). This compound is hydrophobic and serves as a clearing

agent, making the brains transparent. At this stage, the brains were placed in methyl salicylate in a centrally located hole on an aluminum slide. The hole was on both sides covered by cover glass. The brains were examined under a fluorescence light microscope (Leitz Aristoplan, Wetzlar, Germany) to investigate whether the neurons had been successfully stained.

If dye injection had been accomplished, the preparations were rehydrated in a decreasing ethanol sequence (100, 96, 90, 70, 50 %, 10 min each) and treated with PBS (10 min) to rinse out any leftover methyl salicylate. A dehydration procedure in an increasing ethanol sequence was performed to prepare the brains for treatment with the degreasing agent xylol (5 min). Subsequently, the brains were rehydrated in a decreasing ethanol sequence followed by washing in PBS (10 min), before the preparations were immersed in collagenase diluted in PBS (1 mg collagenase: 1 mL PBS) at 36 °C. The preparations were preincubated in normal goat serum (NGS; Sigma, ST. Louis, MO, USA; 10 %) diluted in PBS containing triton X (PBStx; 0.1 %) in room temperature (30 min). Triton X is a detergent, making the plasma membranes more permeable, thus improving access to intracellular antigens. Thereafter, treatment with a monoclonal mouse antibody (SYNORF 1; provided by Prof. E. Buchner, Würzburg, Germany) diluted in PBStx (0.1 %) and NGS (10 %) at 4 °C (48 hours) was performed. This primary antibody labels synapsin, a protein located in presynaptic terminals, and is thus an identifier of synaptic neuropiles. NGS was added to block unspecific binding of proteins. The preparations were subsequently washed in PBS (6 repetitions, 20 min each), after which they were incubated in CY5-conjugated goat anti-mouse secondary antibody (Jackson Immunoresearch; diluted 1:500 in PBStx) at 4 °C (48 hours). CY5 is a hydrophilic fluorescent dye and binds to the primary antibody. After incubation in CY5, the preparations were rinsed in PBS (6 repetitions, 1 hour each) and dehydrated in increasing ethanol concentrations. Finally, the brains were cleared in methyl salicylate and placed in a frontal position on the aluminum slides prepared for confocal laser-scanning microscopy.

2.5 Confocal laser-scanning microscopy

Visualization of stained neurons was performed using a confocal laser-scanning microscope (CLSM) (Leica TCS SP5; Leica Microsystems CMS GmbH, Mannheim, Germany). The brains were scanned with a DPSS laser using a 10x dry objective (HCX PL APO CS), creating a stack of images representing the z-axis of the brain (anterior-posterior axis). The DPSS laser excites at 561 nm, suitable for preparations stained with Micro-Ruby (maximum fluorescence excitation at 550 nm). The beam path setting of the microscope was set to the CY3 option. All scans were

performed with a resolution of 1024x1024 pixels. Axonal and dendritic areas were scanned with a speed of 100-200 Hz, while overview scans of the brains were performed with a scanning speed of 400 Hz. The interslice distance in the z-axis, the z-step size, was automatically set using an optimization formula in the Leica software, yielding step sizes between 2−3.5 µm. The resulting stack of confocal images for each preparation was saved as a Leica Image File (.lif) and converted to Amira Mesh format (.am) in Amira (v. 4.1; Amira Visage Imaging Inc., San Diego, CA, USA). A scaling factor of 1.6 was applied to the image stacks to compensate for the refractive power of the methyl salicylate.

2.6 Three-dimensional reconstruction of a stained neuron and transformation into the standard brain atlas

The raw data provided by the CLSM was used as template to create a three-dimensional model of a selected neuron in the computer software Amira. The neuron was manually reconstructed using a skeleton tool (Schmitt *et al.*, 2004; Evers *et al.*, 2005), tracing the neuronal projections slice by slice in the image stack. After reconstructing the neuron, selected neuropile structures were reconstructed as label images using the segmentation editor in Amira. These label images constituted a reconstruction of the brain preparation, including distinctive neuropile structures (e.g. the mushroom bodies and the anterior optic tubercles) corresponding to structures included in the standard brain atlas (SBA) of this species. The label images were affine- and elastically registered to the corresponding label images of the standard brain, giving the label images of the preparation the same coordinates as those of the standard brain. The parameters obtained by this procedure were applied to the reconstructed neuron when affine- and elastically registering it into the SBA. The result was compared with the confocal images to make sure the neuron was correctly positioned in the SBA. The registration of the reconstructed neuron into the SBA was similar to the procedure described by Brandt *et al.* (2005).

2.7 Neurophysiological analyses

In order to investigate the hypotheses regarding neuronal tuning breadth, GNs were selected for neurophysiological analyses of the spike trains based on the following three criteria:

- The neurons had to be tested for at least five different stimuli (assuring that more than one appendage and stimulus have been tested).
- The neurons had to respond to at least one tastant.
- The appendage mediating the response had to be tested with a mechanosensory control (tactile stimulation).

2.7.1 Response strength analysis

To determine the average spiking frequency of the neuron during each response, a response strength analysis of the spike train was carried out. Spontaneous activity for each neuron was exported as bin-wise (bin length 0.05 s) action potential frequencies (in Hertz) using the event correlation option in Spike2. The spontaneous activity was measured in time intervals of 1.0 s before and after each response. The bin-wise frequencies were imported into Microsoft Excel (Excel 2011, Microsoft Corp., Wa, USA) where they were averaged into one frequency value, representing the spontaneous activity of the neuron. If the spontaneous activity of the neuron changed drastically throughout the recording, two or more frequencies were calculated, reflecting the different spontaneous activities. The responses of each neuron to the given stimuli were exported in a similar manner, with predefined response duration of either 600 or 1200 ms (in cases where the responses were considerably longer, other duration parameters were used). The response durations were set to be identical for all responses from one neuron. Where available, both responses of each repeated stimulus were exported. The mean spontaneous firing frequency was subtracted from each of the frequency bins of the response and bins with higher or lower firing frequencies than the spontaneous activity (the excitatory and inhibitory part of the response, respectively) were averaged separately. Consequently, any inhibitory and excitatory parts of a response were prevented from canceling each other out. Originating from this procedure was a mean deviation value (excitatory and/or inhibitory) from spontaneous activity, defined as the response strength. To inspect whether the response strength was significantly different from the spontaneous activity, a z-score value for each response was calculated (equation 1).

$$z = \frac{\bar{X} - \mu}{\sigma} \quad , \qquad [1]$$

where z is the z-score, $\bar{X}$ is the mean response strength, μ is the mean spontaneous firing rate, and σ is the standard deviation of the spontaneous activity. The response was considered significant for $|z| \geq 2$. To determine if two response strengths were different from each other, a pooled standard deviation estimate was used. Two responses were defined to have different strengths if equation 2 was met.

$$\frac{\left|\bar{X}-\bar{Y}\right|}{s_p} \geq 1, \quad [2]$$

where $\bar{X}$ and $\bar{Y}$ represent the mean response strength of stimuli X and Y, respectively, and s_p is the pooled standard deviation. The pooled standard deviation is given by equation 3.

$$s_p = \sqrt{\frac{\sum_{i=1}^{k}((n_i-1)s_i^2)}{\sum_{i=1}^{k}(n_i-1)}}, \quad [3]$$

where n_i is the size of the *i*th sample, s_i^2 denotes the variance of the *i*th sample, and *k* is the number of different samples to be combined.

Finally, the population of response strengths was tested for normality using the Shapiro-Wilks test.

2.7.2 Response strength correlation analysis

A Spearman correlation analysis (Spearman's ρ) was used to investigate how the response strengths of two modalities were related to one another. The Spearman's correlation coefficient (R_s) was calculated between the paired response strengths of two experimental stimuli (mechano/sucrose, mechano/quinine, mechano/NaCl, sucrose/quinine, sucrose/NaCl, quinine/NaCl). Since each response produced an excitatory and inhibitory mean deviation value, only the part (excitatory or inhibitory) yielding a significant response ($|z| \geq 2$) was used in this analysis. Furthermore, because a stimulation causing no response consisted of both excitatory and inhibitory non-significant deviation values, the response strengths of these stimulations were defined as 0. First, the correlation analysis was performed for all stimulations across neurons, irrespective of which appendage generated the response. Thereafter, potentially correlated activity was examined with respect to the different appendages, treating stimulations at the left antenna, the proboscis and the right antenna separately. Finally, response strengths elicited by stimulating different appendages with the same modality was investigated for correlated activity, e.g. the correlation of sucrose stimulation between the left antenna and the proboscis. Before

calculating the correlation coefficient, the response strengths of stimuli X and Y were ranked, converting them into to the set of ranks x and y. The correlation coefficient was then calculated using the ranks (equation 4).

$$R_{x,y} = \frac{\sum_{i=1}^{n}(x_i - \bar{x})(y_i - \bar{y})}{\sqrt{\sum_{i=1}^{n}(x_i - \bar{x})^2}\sqrt{\sum_{i=1}^{n}(y_i - \bar{y})^2}}, \quad [4]$$

where $R_{x,y}$ is the Spearman correlation coefficient between the ranks of x and y, $\sum_{i=1}^{n}(x_i - \bar{x})(y_i - \bar{y})$ is the covariance between x and y, and $\sqrt{\sum_{i=1}^{n}(x_i - \bar{x})^2}\sqrt{\sum_{i=1}^{n}(y_i - \bar{y})^2}$ is the product of the standard deviations of x and y. $\bar{x}$ and $\bar{y}$ denote the mean of the ranks of x and y, respectively. To test if the correlations were statistically significant, i.e. rejecting the null hypothesis ($R_s = 0$), a permutation test using Matlab (v. R2011b, TheMathWorks.inc, Natick, Massachusetts, USA) was performed. The significance level (α) was set to 5 %.

2.7.3 Response frequency analysis

In order to investigate the temporal expression of a response, a frequency spectrum analysis was carried out. This analysis produces a spectrum showing the individual spiking frequencies constituting the response, i.e. the particular frequencies at which the neuron emitted action potentials during the response. A frequency spectrum was computed for each response and for an appurtenant spontaneous activity. This was done in order to distinguish the dominant frequencies of the response from those of the spontaneous activity. The spike trains, from which the spectra were produced, were exported from Spike2 as waveform audio files (.wav). The files were imported into Matlab, where a Lomb-Scargle signal transformation algorithm was executed to create the spectra. The Lomb-Scargle algorithm (Press *et al.*, 1992) applies the same principles as the more widely used Fast Fourier Transform (FFT) algorithm, but the former was chosen due to its higher sensitivity. In essence, the Fourier and Lomb-Scargle transformations state that any signal in time can be represented as a sum of sine waves of different frequencies and phases. The frequency spectrum produced is thus a measure of the contribution from different sine wave frequencies in constituting the original signal (Bloomfield, 2000).

In addition, the common FFT algorithm was applied to all responses and a representative spontaneous activity from each neuron. The FFT frequency spectrum of the spontaneous activity was subsequently subtracted from the FFT frequency spectrum of the response, yielding a spectrum reflecting the spike frequency differences between the neuron in the active state and at rest. This was subsequently color plotted and scaled, enabling a comparison between color spectra from different responses. The color spectrum of each response was scaled according to the neuron's activity level at each particular frequency relative to mean spontaneous activity. Shades of red represented degrees of increased activity, ranging from average spontaneous activity (white) to 20 times increased activity (dark red). Shades of blue represented decreased activity from average spontaneous activity to 20 times decreased activity (dark blue). A filter was set at 50 Hz intervals (50, 100, 150, 200, 250, 300 Hz) making these specific areas appear white. The filtering was performed due to the appearance of electrical artifacts at these frequencies, resulting from the influence of local electrical lines on intracellular recordings (Pei and Tseng, 1995). The Matlab code that generated the FFT color plots is available in appendix I.

3 Results

In this study, intracellular recordings were carried out from 44 protocerebral GNs in the moth *H. virescens* (five recordings were provided by Dr. Pål Kvello). These neurons were tested with mechanosensory and three gustatory stimuli applied to both antennae and the proboscis. Over the population of 44 neurons, 289 different stimulations were carried out. Among them, a preliminary qualitative analysis revealed a total of 102 responses (excitation/inhibition). In addition, when a stimulus evoked a response, that stimulation was repeated. However, only one of the two responses from the repeated stimuli is accounted for among the 102 responses. Table 1 shows the number and percentage of the excitatory and inhibitory responses out of the total 102 responses. Among the 44 neurons, 11 were stained, some of them incompletely or co-stained with other neurons in the same preparation. The neurons varied in their responses to both stimulus identity (modality) and application site (appendage). In order to investigate the neuronal tuning breadth, GNs were selected for further analyses based on the criteria defined in section 2.7: Neurophysiological analyses.

Table 1. Excitatory and inhibitory responses from 44 neurons triggered by stimulation with sucrose, quinine, NaCl and tactile touch (mechano).

	Number of responses		**Percentage (%)**	
	Excitation	*Inhibition*	*Excitation*	*Inhibition*
Sucrose	22	18	21.57	17.65
Quinine	20	12	19.61	11.76
NaCl	12	4	11.76	3.92
Mechano	6	8	5.88	7.84
Sum	***60***	***42***	***58.82***	***41.18***
Sum total	102		100	

3.1 Physiological properties of protocerebral GNs

Among the 44 neurons, 30 fulfilled the criteria for further analyses. However, four neurons contained solely responses that did not meet the z-score criterion of $|z| \geq 2$, and were discarded. The remaining 26 recordings were gathered from 21 moths, with maximum two recordings in one preparation. Eight neurons were stained, one of which was fully reconstructed and registered into the SBA. From the population of 26 GNs, three different classes of protocerebral GNs appeared, differing in their response tuning breadth to stimulus identity and application site:

- Class 1 GNs responded to a single tastant applied at a single appendage.
- Class 2 GNs responded to two or more stimuli applied at a single appendage.
- Class 3 GNs responded to two or more stimuli applied at two or three appendages.

3.1.1 Response profiles

Because of the limited time duration of the challenging intracellular recordings, every neuron was not tested with the complete protocol of stimuli. Thus, it should be taken into account that the groups and the number of neurons within these groups could have changed with ampler testing.

The 26 neurons demonstrated pure excitation or inhibition and no mixed responses were present. Among the 26 neurons, a total of 13 (50 %) were categorized as class 1 GNs. Seven of them responded to sucrose, four to quinine and two to NaCl. The response profiles of class 1 GNs are illustrated in Fig. 1 (A). Altogether, the neurons in this class were tested for 106 out of 156 possible stimuli, resulting in an overall stimulation score of 68 %. The neurons responding to sucrose showed both excitatory and inhibitory responses. The excitation was mediated by the proboscis in GN 1, 2, and 3, and by the right antenna in GN 6 and GN 7. The excitatory response of GN 1 is presented in Fig. 2. Two neurons (GN 4 and GN 5) responded with inhibition mediated by the proboscis. GN 8 and GN 9 responded by excitation to NaCl stimulation of the left antenna. The neurons responding to quinine stimulation of the antennae showed both excitatory (GN 11, 12 and 13) and inhibitory (GN 10) responses.

Seven neurons (27 %) fitted into class 2 GNs. The response profiles of these neurons are illustrated in Fig. 1 (B). Altogether, the seven neurons were tested for 51 out of 84 possible stimuli, resulting in an overall stimulation score of 61 %. In these neurons, the gustatory stimuli elicited the same response mode, either excitation or inhibition. Moreover, all of them responded

to stimulation with both sucrose and quinine: with excitation in GN 14, 15, 16, 18, and inhibition in GN 17, 19 and 20. Among the four neurons tested for NaCl, GN 15 and GN 18 were excited, GN 19 was inhibited, and GN 16 did not respond. Responses to tactile stimulation were evident in two neurons (GN 17 and GN 18), wherein the mechanosensory response mode was opposite of the taste response mode. This is exemplified in Fig. 3, showing spike trains from GN 17 in response to mechanosensory and gustatory stimulation of the left antenna.

Six neurons (23 %) were categorized according to the class 3 specifications, responding to different stimuli applied to two or three appendages. The response profiles of the six class 3 neurons are illustrated in Fig. 1 (C). Altogether, the neurons in this class were tested for 63 out of 72 possible stimuli, yielding an overall stimulation score of 88 %. GN 21 demonstrated the broadest tuning by responding to all presented stimuli, mainly by inhibition. The responses of GN 21 to mechanosensory and gustatory stimulation are shown in Fig. 4. The most broadly tuned neuron with solely excitatory responses was GN 26. This neuron was excited by the three gustatory stimuli applied to the left antenna and the proboscis. GN 25 displayed the narrowest tuning in this group, excited by sucrose application to the right antenna and quinine application to the proboscis. Three neurons (GN 21, 23 and 24) were similar in that they showed mechanosensory responses of opposite mode to their excitatory taste responses. However, they differed in their excitatory responses. GN 21 responded to quinine stimulation of the proboscis, GN 23 to quinine stimulation of the proboscis and sucrose stimulation of the right antenna, and GN 24 to sucrose stimulation of the proboscis and the right antenna. Unfortunately, GN 24 was not tested for mechanosensory stimuli applied to the proboscis, and GN 21 for mechanosensory stimuli applied to the right antenna. Consequently, it cannot be ruled out that the responses elicited by stimulation of these appendages were evoked by the mechanosensory component of the stimulation. Interestingly, no neurons showed excitatory responses mediated by stimulation of both the antennae, only inhibitory responses were obtained (GN 21 and GN 22). Stimulating the right antenna with sucrose, quinine and NaCl, and the left antenna with quinine evoked the inhibitory responses in GN 22.

3.1.2 Spontaneous activity

The three classes of GNs differed slightly in their average spontaneous activity. Whereas the majority of class 1 neurons at rest fired action potentials between 0 and 20 spikes/s (Hz), class 2 and 3 neurons had on average higher spontaneous firing rates. The majority of the class 2 neurons (71 %) had an average spontaneous activity between 18 and 42 Hz, and 67 % of class 3 neurons between 34 and 70 Hz. Among the 26 neurons, only GN 11 (class 1) exhibited no spontaneous activity. Some neurons in class 1, 2 and 3 showed tonic firing mode, whereas others exhibited regular or irregular bursting activity. Hence, a temporal feature characterizing the spontaneous activity of each class did not appear.

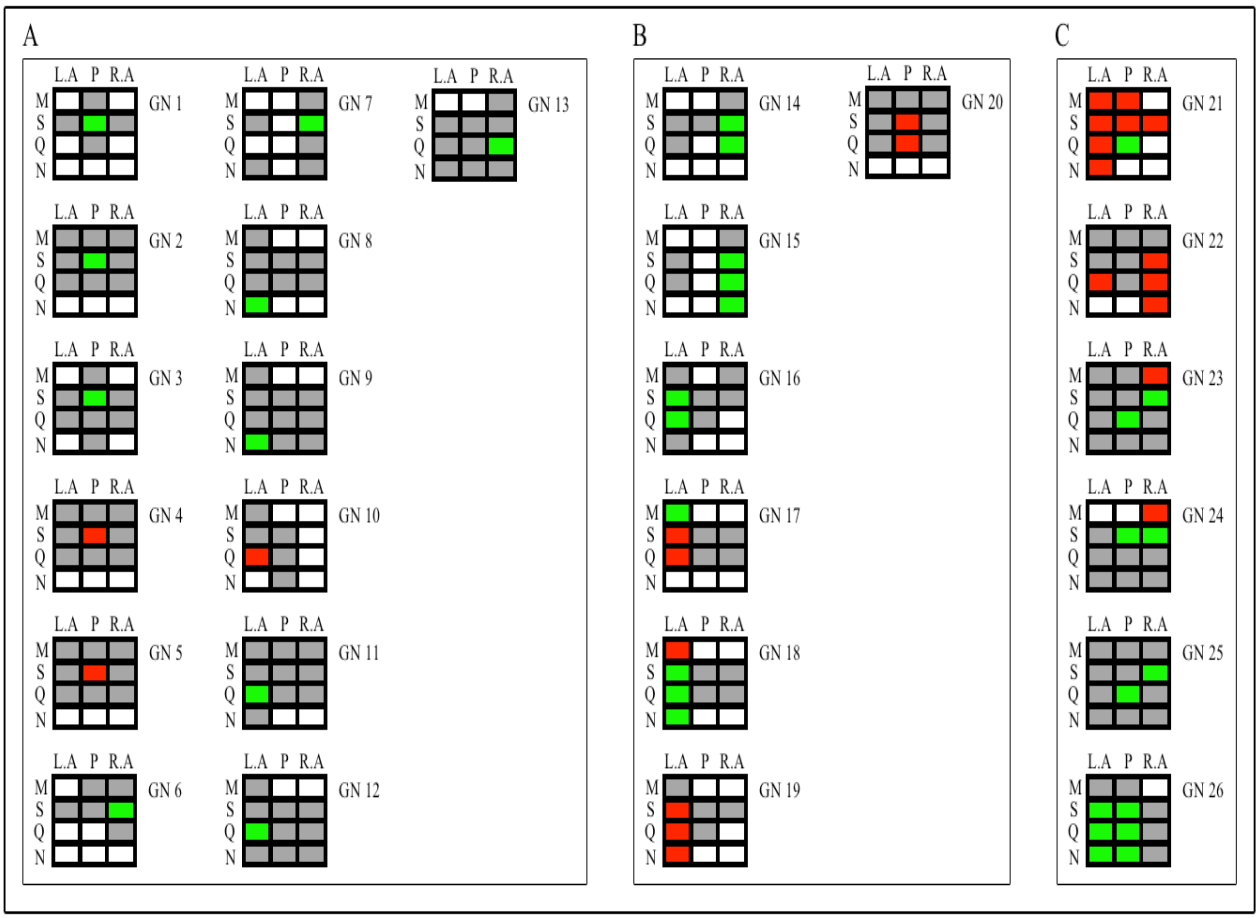

Figure 1. Response profiles of the 26 neurons analyzed in this study. Figure A, B and C show class 1, 2 and 3 GNs, respectively. GN = Gustatory Neuron. In the response profile of each neuron, a column represents one appendage (L.A = Left antenna, P = Proboscis, R.A = Right antenna) and a row represents one modality (M = Mechano, S = Sucrose, Q = Quinine, N = NaCl). Green, red, grey and white fields indicate excitation, inhibition, no response and not tested, respectively.

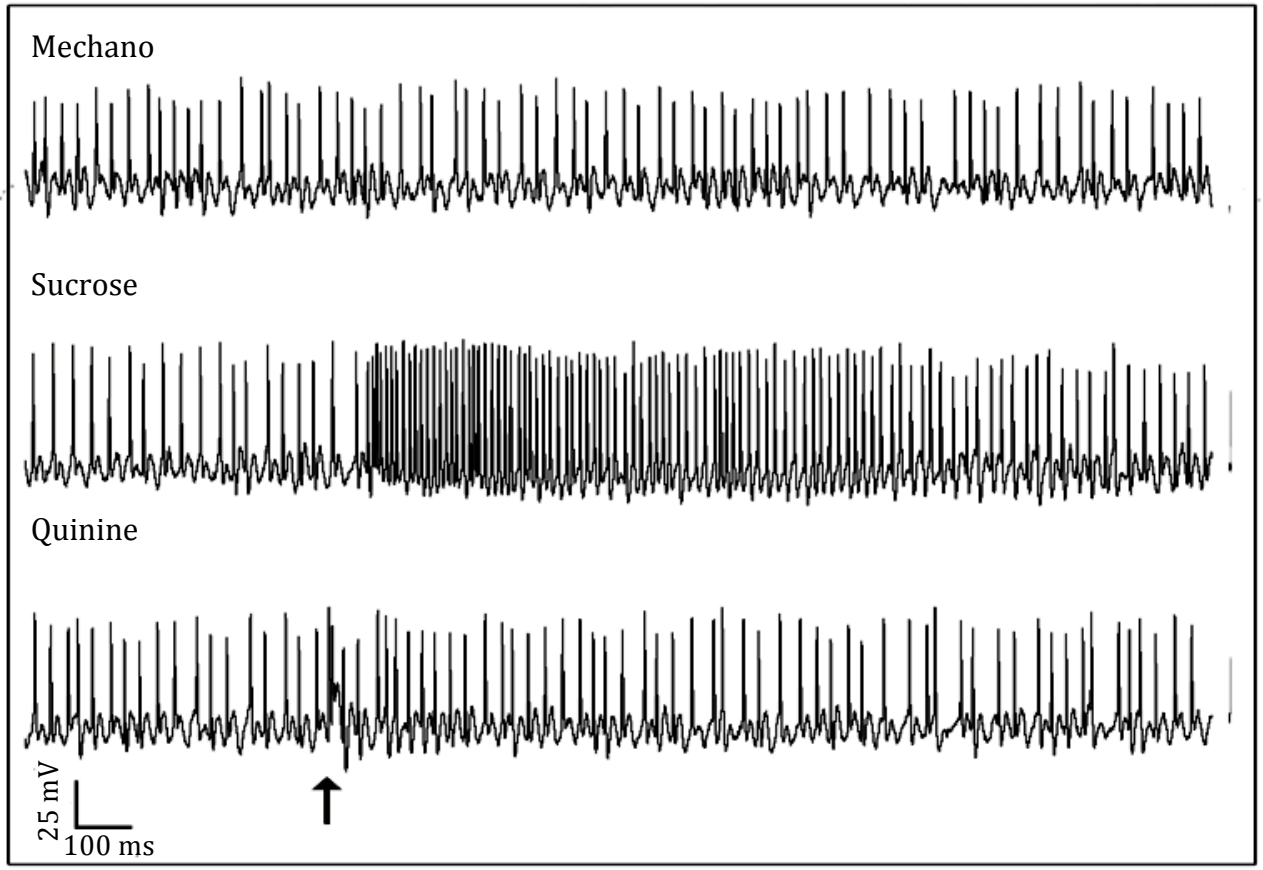

Figure 2. Spike trains from a class 1 neuron (GN 1) stimulated at the proboscis with mechano, sucrose and quinine. The arrow indicates stimuli onset.

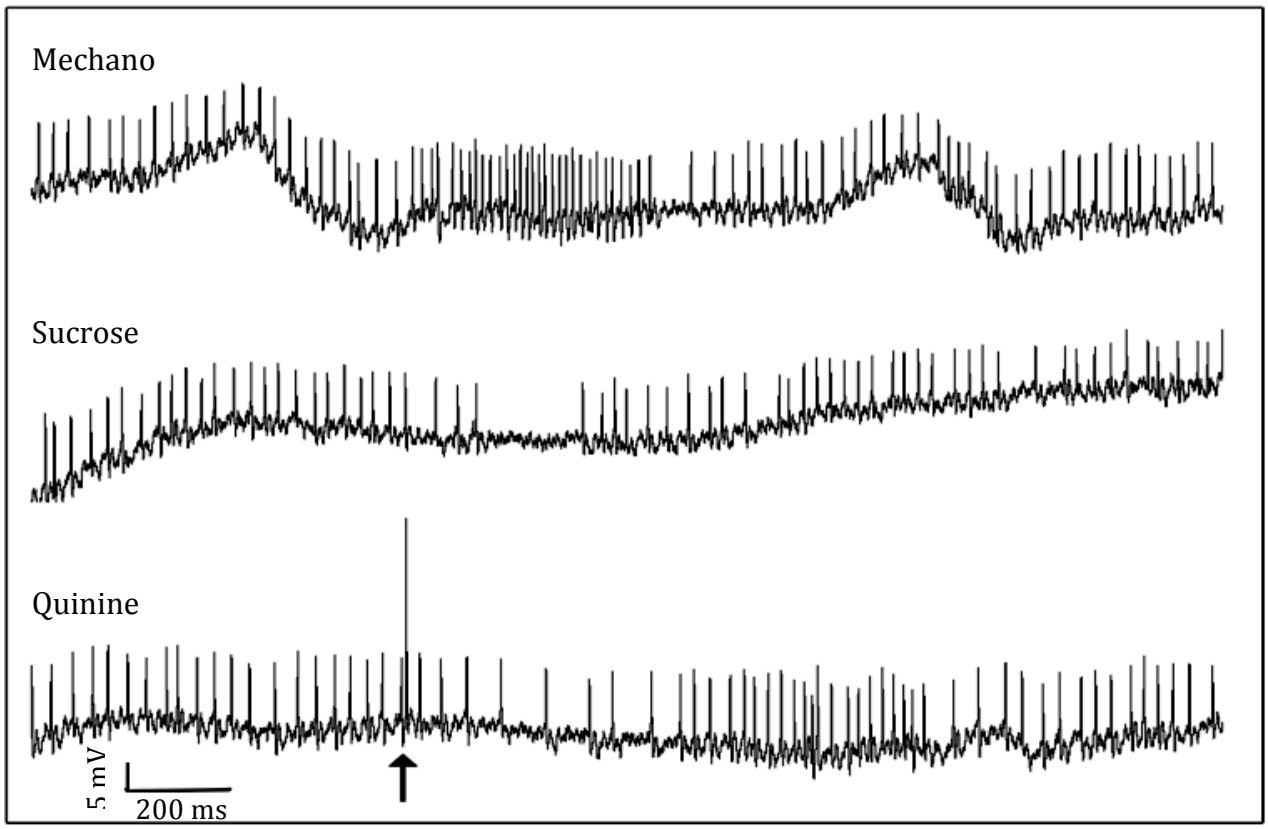

Figure 3. Spike trains from a class 2 neuron (GN 17) stimulated at the left antenna with mechano, sucrose and quinine. The arrow indicates stimuli onset.

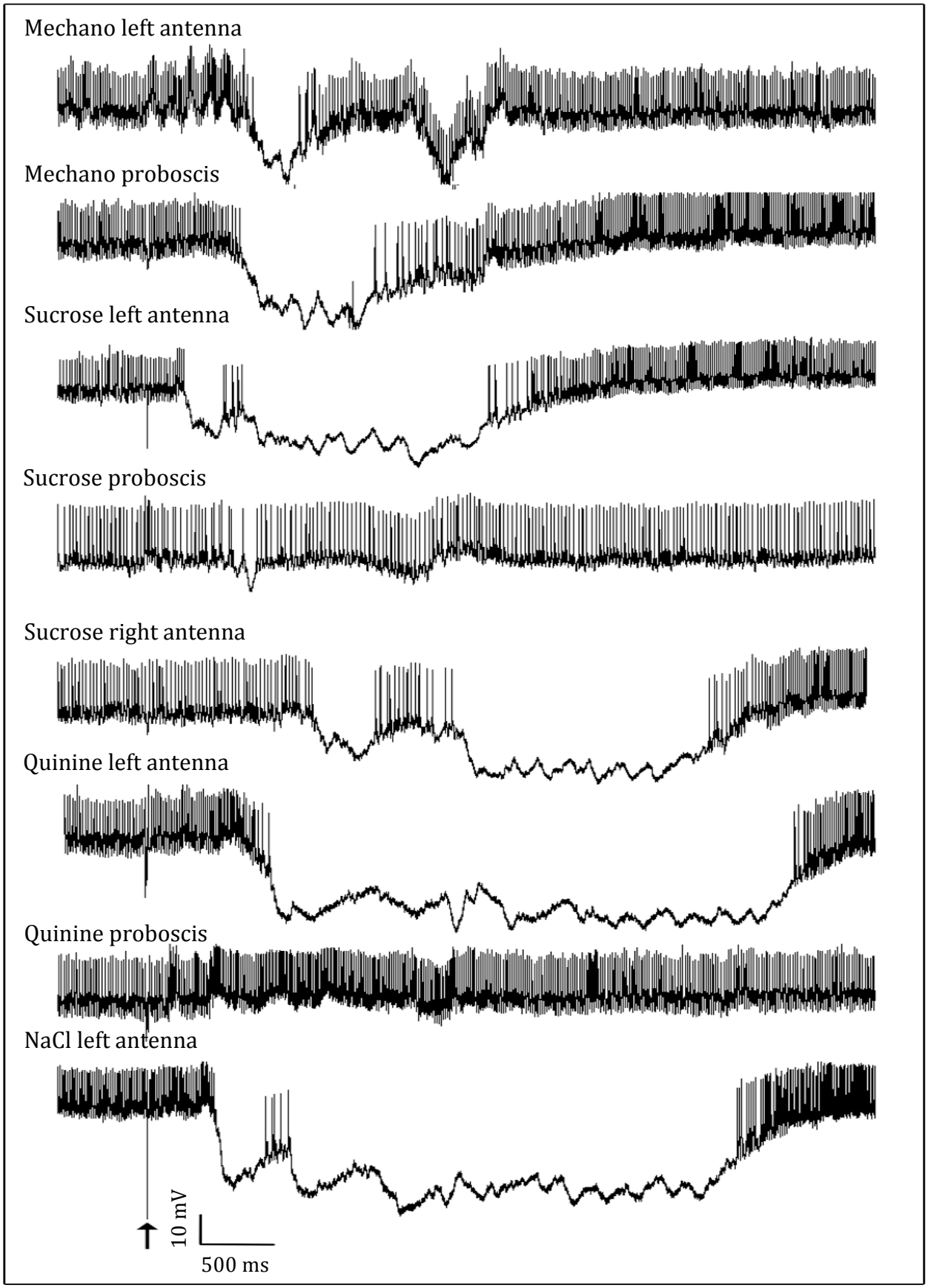

Figure 4. Spike trains from a class 3 neuron (GN 21) stimulated at the left antenna with mechano, sucrose, quinine and NaCl, the proboscis with mechano, sucrose and quinine, and the right antenna with sucrose. The arrow indicates stimuli onset.

3.1.3 Response strength

The class 1 neurons exhibited a large array of response strength values, illustrated in Fig. 5. The two NaCl responding GNs showed excitatory response strengths of 10 and 16 Hz, whereas sucrose and quinine responding neurons showed excitatory strengths from 12-59 Hz and 19-62 Hz, respectively. The response strengths of the two neurons responding by inhibition to sucrose stimulation were 7 and 26 Hz, whereas the neuron responding by inhibition to quinine stimulation had a response strength of 11 Hz. The response strength analysis of the class 2 neurons yielded excitatory responses from 11-32 Hz and inhibitory responses from 8-30 Hz. The response strength values of the individual class 2 neurons are presented in Fig. 6. The difference in response strength between taste modalities in a single neuron ranged from 1-12 Hz, whereas the strength differences between gustatory and mechanosensory stimuli were larger, with opposite modes. The class 3 neurons showed excitatory response strength values from 19-99 Hz, the majority from 19-67 Hz. The strength of the inhibitory responses ranged from 11-53 Hz. The response strength values of the individual class 3 neurons are presented in Fig. 7. As opposed to class 2 neurons, class 3 neurons expressed considerably larger span in response strength values between modalities within a single neuron. This is exemplified in GN 25 (Fig. 7), showing a difference of approximately 70 Hz between responses elicited by stimulation of sucrose applied to the right antenna and quinine applied to the proboscis.

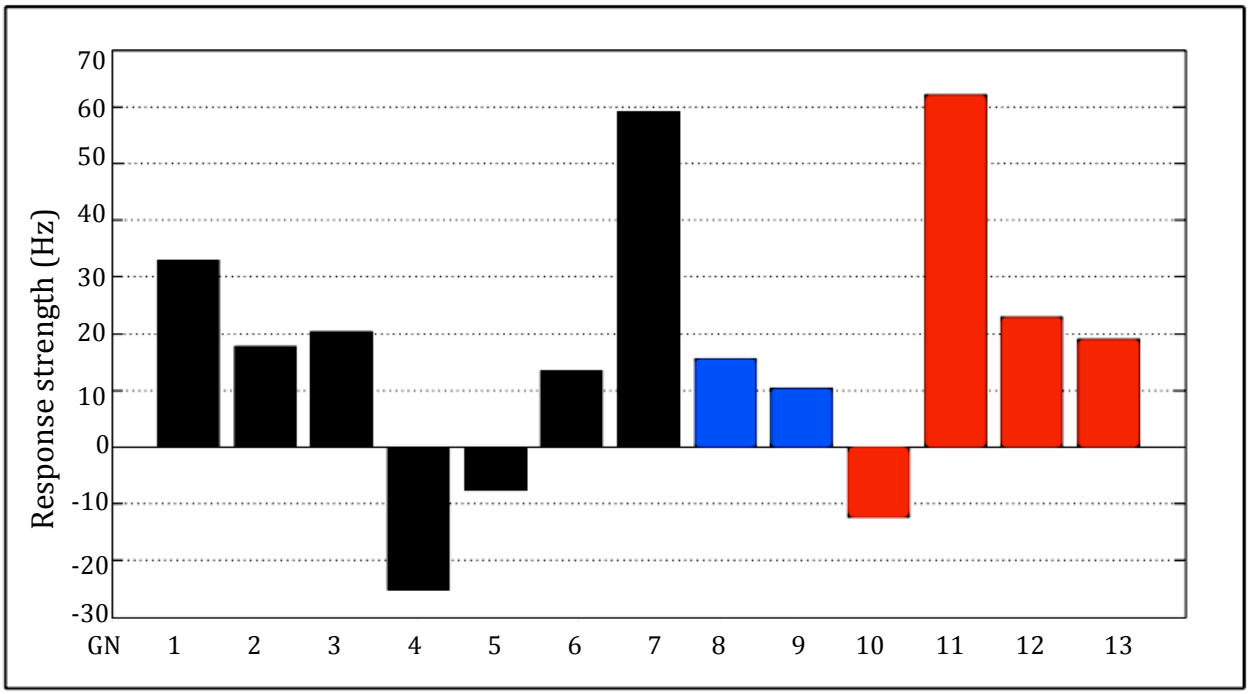

Figure 5. Response strengths of the 13 neurons included in the class 1 category. The bars, colored black, blue and red, represent neurons responding to sucrose, NaCl and quinine, respectively. The 0 Hz line indicates mean spontaneous activity. Positive and negative frequency values represent excitation and inhibition, respectively.

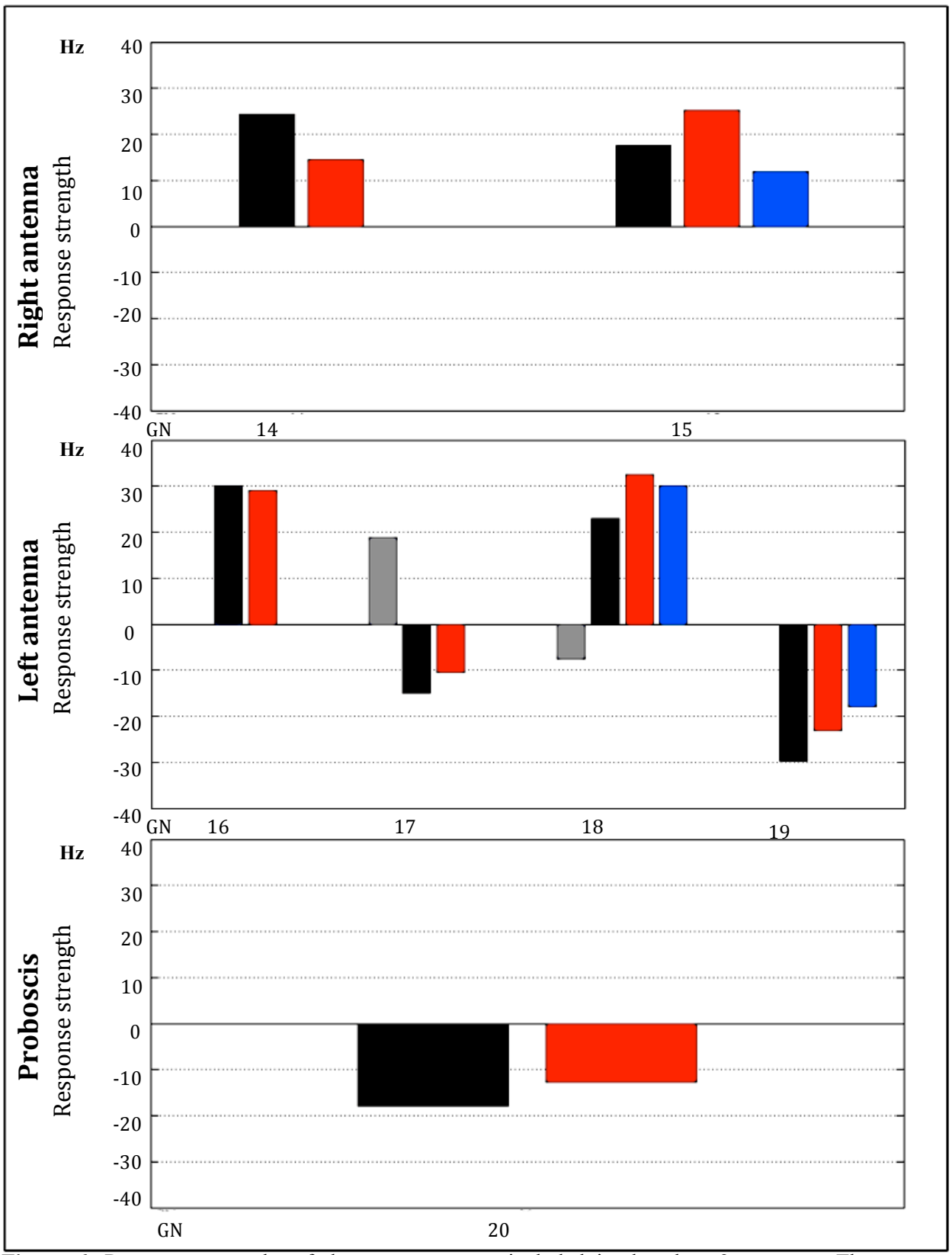

Figure 6. Response strengths of the seven neurons included in the class 2 category. The neurons responding to stimulation of the right antenna (top diagram), the left antenna (middle diagram) and the proboscis (bottom diagram) are presented separately. The bars, colored grey, black, red and blue, represent responses to mechano, sucrose, quinine and NaCl, respectively. The 0 Hz line indicates mean spontaneous activity. Positive and negative frequency values represent excitation and inhibition, respectively. Empty slots indicate no response or not tested, cf. Fig. 1 (B).

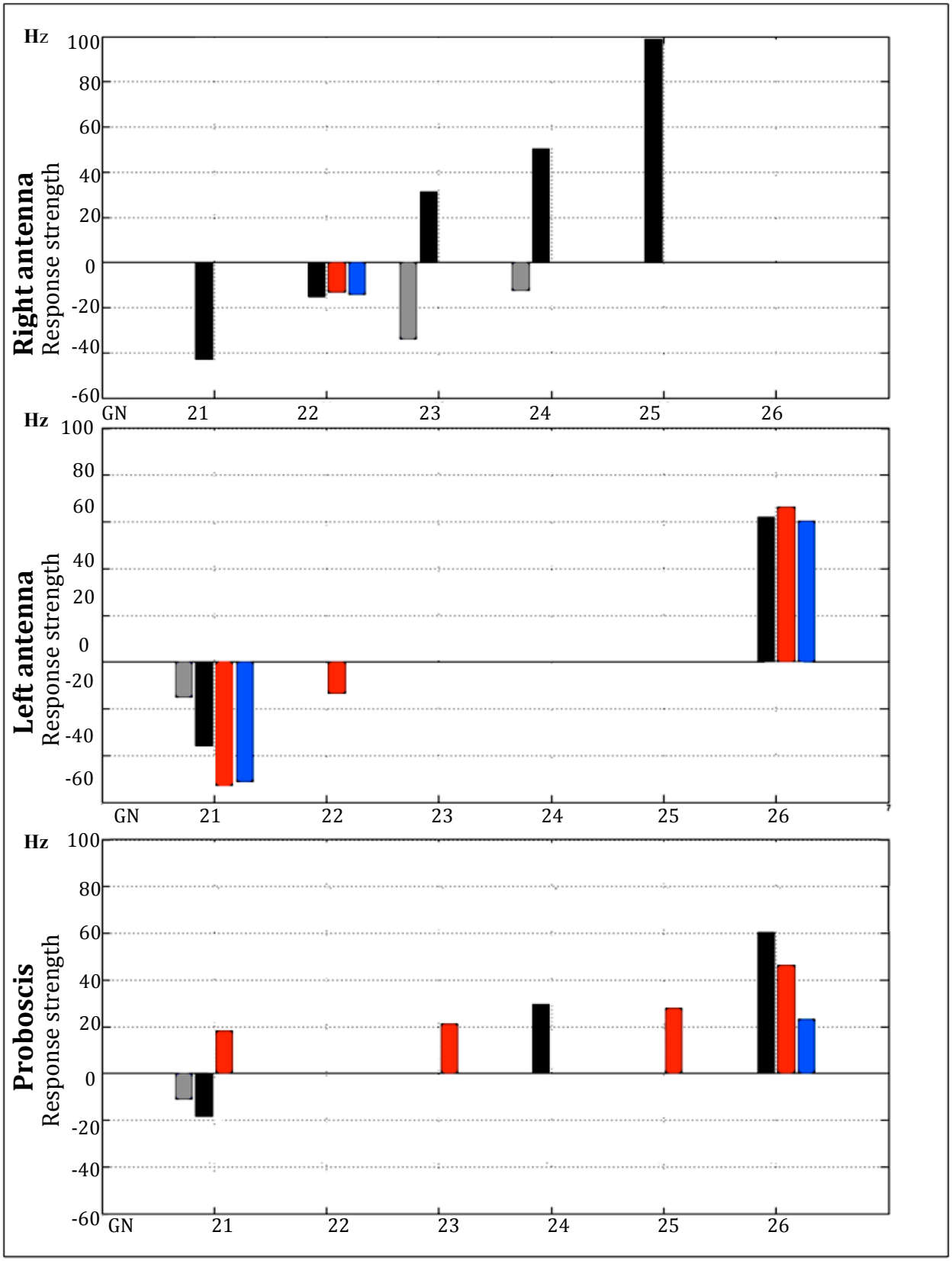

Figure 7. Response strengths of the six neurons included in the class 3 category. Responses from each neuron are presented according to the appendage mediating the response. The top, middle and bottom diagram represent the right antenna, the left antenna and the proboscis, respectively. The bars, colored grey, black, red and blue, represent responses to mechano, sucrose, quinine and NaCl, respectively. The 0 Hz line indicates mean spontaneous activity. Positive and negative frequency values represent excitation and inhibition, respectively. Empty slots indicate no response or not tested, cf. Fig. 1 (C).

3.1.4 Response strength correlation

In order to investigate how strongly the response strengths of different stimuli are related, a Spearman rank correlation analysis was performed. This correlation, in contrast to the Pearson product-moment correlation, does not assume that the experimental data is normally distributed. The population of response strengths in this study was not normally distributed (Shapiro-Wilks test, $p < 0.05$). Consequently, the Spearman rank correlation was preferred. The analysis was carried out over the whole population of 26 neurons without respect to the different classes of GNs. First, the response strengths were analyzed without regard to which appendage mediated the response. This resulted in significant positive correlations (two tail permutation test, $\alpha = 0.05$) between the response strengths of each pair of tastants: sucrose/quinine ($R_s = 0.47$, $N = 66$, $p < 0.001$), sucrose/NaCl ($R_s = 0.56$, $N = 32$, $p < 0.001$), quinine/NaCl ($R_s = 0.65$, $N = 31$, $p < 0.001$). These correlations mean that an increase or decrease in response strength to stimulation with one tastant would tend to be accompanied by an increase or decrease in response strength to the other tastants. The response strengths between tactile stimulation and the three gustatory stimuli were not significantly correlated. No significant negative correlations were detected, meaning that no relationship existed where a change in response strength to stimulation with one tastant was accompanied by an opposite change in strength to another tastant. This means that no excitatory responses to stimulation of one tastant tended to be accompanied by an inhibitory response to stimulation of another tastant.

Second, the correlations were calculated with respect to which appendage mediated the response, investigating correlated activity between responses mediated by the same appendage. This uncovered that the relationships were not uniform across the three appendages. Regarding responses mediated by the left antenna, the response strengths to sucrose stimulation were significantly correlated with quinine ($R_s = 0.80$, $N = 23$, $p < 0.001$) and NaCl ($R_s = 0.89$, $N = 14$, $p < 0.001$). Moreover, a positive significant correlation was observed between quinine and NaCl ($R_s = 0.66$, $N = 13$, $p < 0.05$). Regarding responses mediated by the proboscis, no significant correlations were observed. In contrast, the response strengths of quinine and NaCl mediated by the right antenna were significantly correlated ($R_s = 0.86$, $N = 10$, $p < 0.01$).

Third, considering the relation between the response strengths elicited by the same modality applied at different appendages, no significant correlations were found between responses to sucrose mediated by the left antenna/proboscis, left antenna/right antenna and proboscis/right antenna. Similarly, no correlated activity was found for responses to quinine mediated by the

three appendages. Response strengths to NaCl were not significantly correlated between left antenna and proboscis, whereas insufficient experimental testing rendered it not possible for further correlation analysis of NaCl.

In summary, the findings from the correlation analysis showed a high degree of correlated activity between the strengths of tastant-evoked responses mediated by the left antenna (three correlations), not a single correlated pair of responses mediated by the proboscis, whereas the right antenna mediated one correlated pair of response strengths. Furthermore, no correlations were found between the responses elicited by stimulating two appendages with the same modality.

3.1.5 Discrimination of stimuli by class 2 and 3 GNs

Resulting from the high specificity of class 1 neurons, a stimulus-evoked response would provide information about both the identity and the location of the applied stimulus. In contrast, this relation was not as straightforward in the broadly tuned class 2 and 3 neurons, which responded to several stimuli. Nevertheless, differences in response strengths or temporal patterns produced by individual class 2 and 3 GNs might contribute to discrimination between taste modalities and their application sites.

3.1.5.1 Response strength

The responses evoked in a single neuron were classified as having different average strengths based on a pooled standard deviation estimate. Responses referred to in the following text have been defined as different or not different using this method.

Among the class 2 neurons, three neurons (GN 14, 17 and 20) responded stronger to sucrose than to quinine, and GN 19 responded stronger to sucrose than to quinine and NaCl. The others, GN 15, 16 and 18, showed no differences in response strengths between the taste modalities. The response strengths of class 2 GNs are presented in Fig. 6. Class 3 neurons expressed more complex response profiles compared to class 2 neurons. Whereas both class 2 and 3 neurons responded in an unspecific manner regarding stimulus identity, class 3 neurons were less specific concerning stimulus application site (Fig. 1). The response strengths of class 3 GNs are presented in Fig 7. Among the eight responses mediated by the three appendages in GN 21, NaCl and quinine application to the left antenna resulted in the strongest inhibition (Fig. 4). Furthermore, the inhibitory responses evoked by stimulation of the antennae with gustatory stimuli were stronger than those mediated by the proboscis. GN 22 responded with the strongest

inhibitory response to sucrose application to the right antenna, while no distinction could be made between the responses evoked by quinine and NaCl stimulation. Both GN 23 and GN 25 responded stronger to sucrose applied at the right antenna than quinine applied at the proboscis. GN 24 responded with different excitatory strengths to sucrose application to the proboscis and the right antenna, showing a preference for the antennal stimulation. GN 26 showed no discernible differences between the excitatory responses evoked at the left antenna. However, the excitatory responses mediated by the left antenna were stronger than those elicited by NaCl stimulation of the proboscis.

3.1.5.2 Temporal firing characteristics

The response frequency analysis aimed at detecting the frequency distribution of the response. The Lomb-Scargle and Fourier analyses of single cell responses were conducted on seven of the eight class 2 and 3 neurons (GN 14, 15, 16, 23, 24, 25, 26) displaying excitatory responses to gustatory stimulation. The frequency analysis method is vulnerable to disturbance and background noise in the recording. Because abundant noise and interference were present in the recording of GN 18, it was not included in the analysis. The response frequency analysis uncovered conspicuous differences in firing rate dynamics between the excitatory responses elicited by different stimuli. The diversity in frequency distribution was a distinctive feature of the responses from the seven class 2 and 3 neurons analyzed, and is exemplified in the following text by GN 26 (Fig. 8 and 9). In the spontaneous activity state, GN 26 fired action potentials mainly at 35-40 Hz, but it also showed activity in the frequency interval from 60-110 Hz (appendix II, Fig. 15). The average spontaneous activity of GN 26 was estimated to approximately 60 Hz. A notable difference in spiking activity between the spontaneous activity and the responses of GN 26 was the almost complete lack of activity in the 0-50 Hz interval in the responses (Fig. 9). Bear in mind that the response frequencies referred to in the following text are absolute frequencies, not relative to spontaneous activity. In the response elicited by sucrose application to the proboscis, GN 26 fired predominantly at frequencies of 120 and 140-150 Hz (Fig. 9: A), whereas the response elicited by sucrose stimulation of the left antenna predominantly consisted of frequencies of 90, 140-150 and 175-180 Hz (Fig. 9: B). The two quinine responses displayed activity in the range 80-180 Hz. In this frequency interval, the response mediated by the proboscis consisted predominantly of frequencies of 80, 90 and 175 Hz (Fig. 9: C), whereas the response mediated by the left antenna largely contained frequencies of 110, 130-135 and 160 Hz (Fig. 9: D). The response elicited by NaCl stimulation of the proboscis was transmitted principally at a frequency of 80 Hz, although additional higher frequency

activity was present (Fig. 9: E). In contrast, the response evoked by stimulation of the left antenna with NaCl was transmitted mainly by frequencies of 90-100 and 160-175 Hz (Fig. 9: F). In summary, these six responses displayed clear differences in spike discharge patterns (Fig. 8), each response producing a distinct frequency distribution (Fig. 9). It is also noteworthy that two repetitions of the same stimulus produced two responses with different frequency distributions (Fig. 10). Furthermore, a recurring feature of the recorded protocerebral GNs was that the first stimulation of a taste modality typically produced a stronger (high frequency) excitation than the second stimulation (Fig. 11).

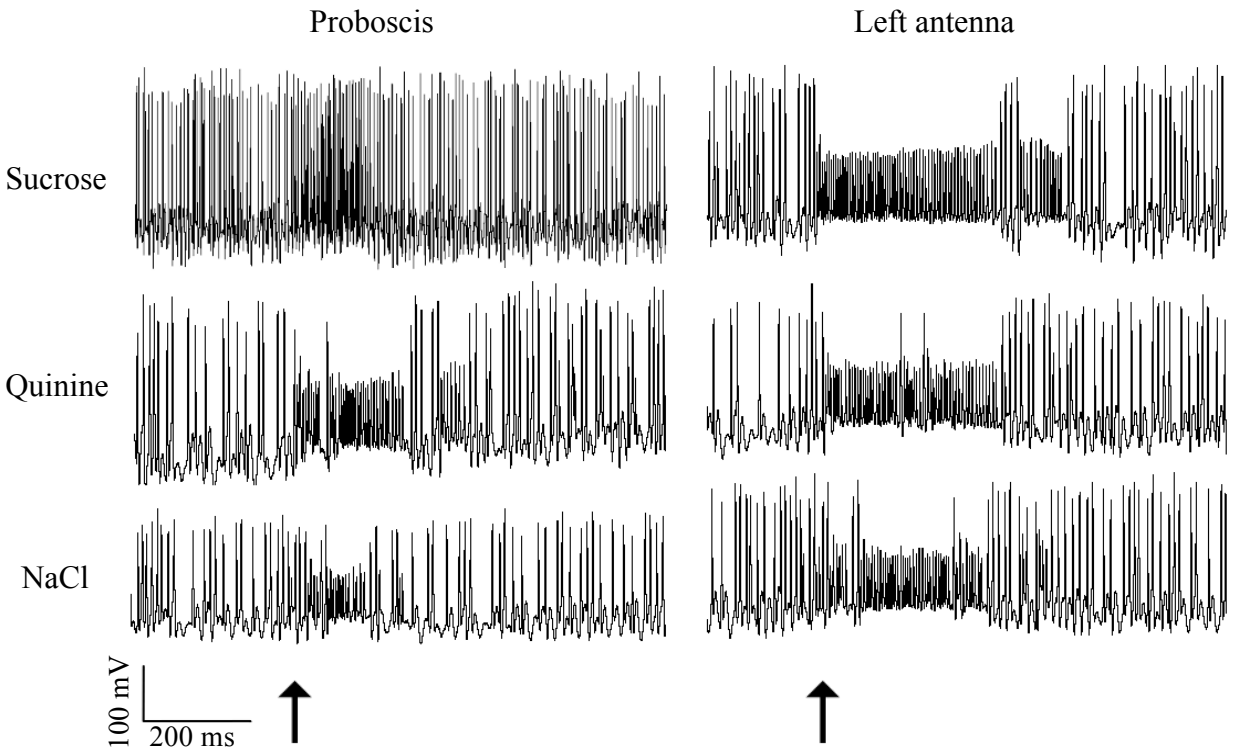

Figure 8. Spike trains from GN 26 in response to stimulation with sucrose, quinine and NaCl applied at the proboscis and the left antenna. Left column shows responses to sucrose, quinine and NaCl mediated by the proboscis and the right column shows responses to the same stimuli mediated by the proboscis. The arrows indicate stimuli onset.

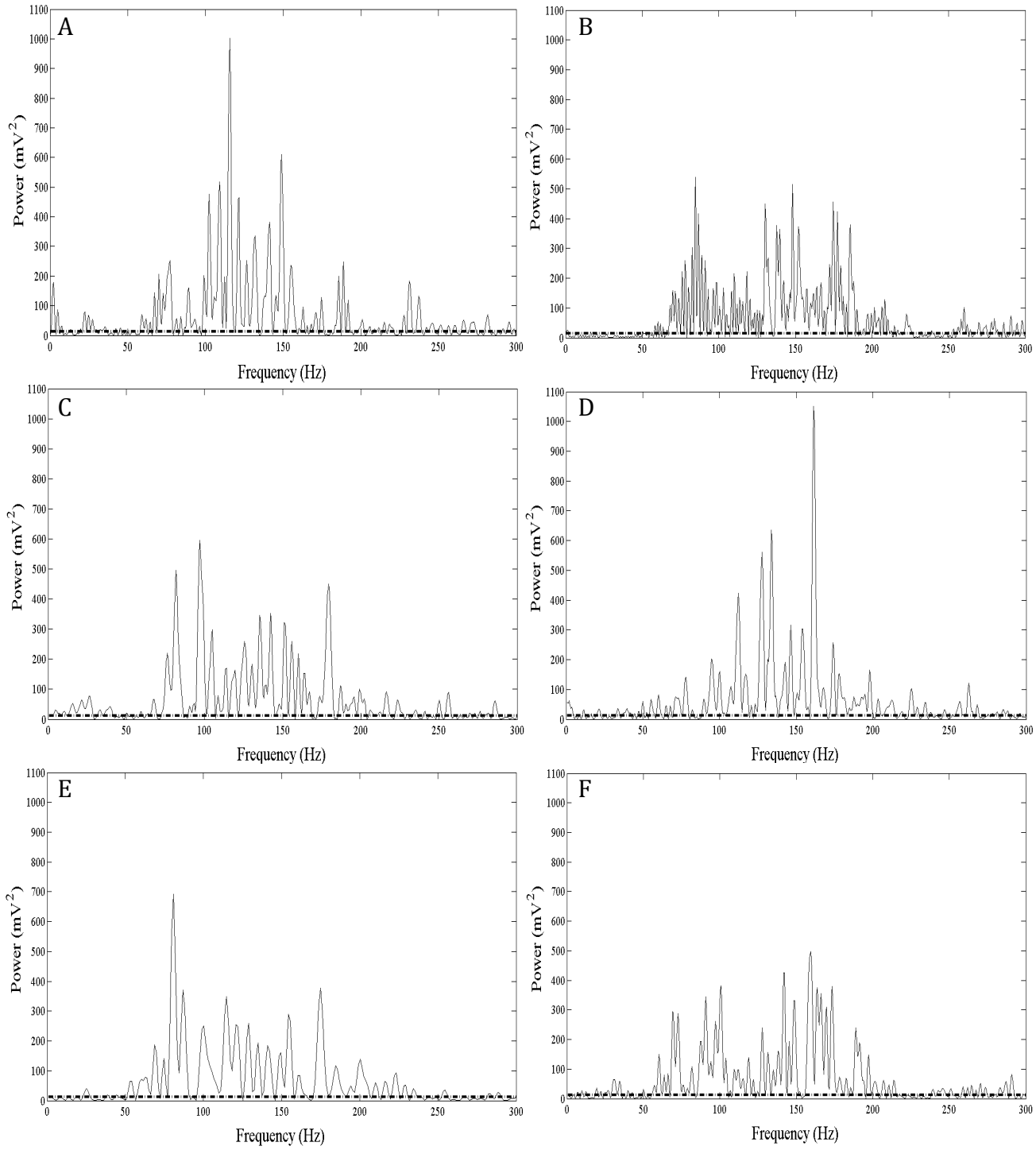

Figure 9. Lomb-Scargle frequency spectra of gustatory responses from GN 26 stimulated at the proboscis (left column) and left antenna (right column) with sucrose (A, B), quinine (C, D) and NaCl (E, F). Note that activity at exactly 0, 50, 100, 150, 200, 250, 300 Hz is not regarded as neuronal spiking activity, since electrical artifacts are present at these frequencies due to the influence of local electrical power lines.

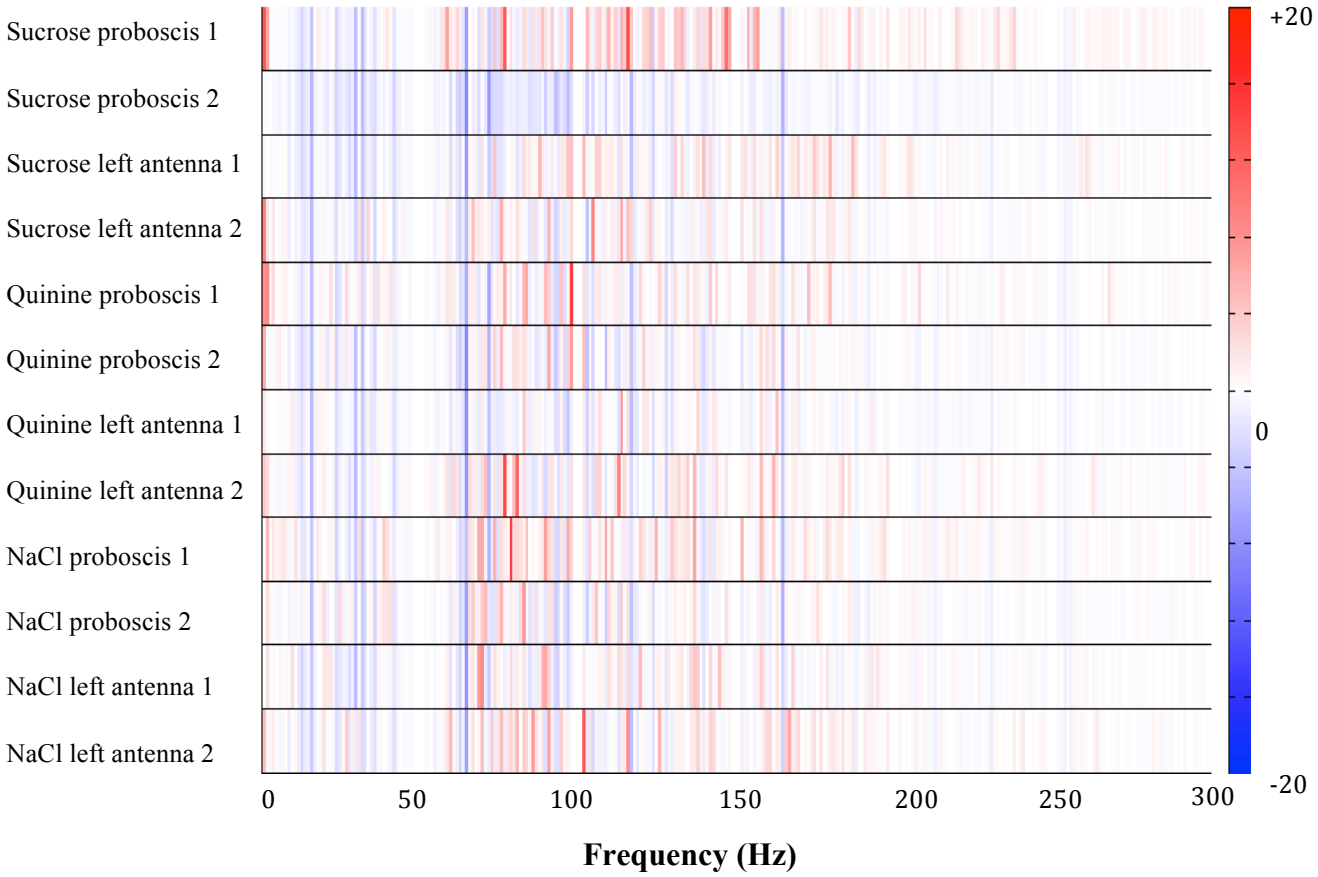

Figure 10. Colorized net frequency spectra of responses from GN 26. The spectra labeled "1" and "2" represent the responses to the first and second stimulation, respectively. Note the differences between the frequency spectra of responses elicited by stimulation with the same modality. The responses labeled "1" is the same response used to generate the corresponding Lomb-Scargle spectrum in Fig. 8. Red and blue colors indicate increased and decreased activity, respectively, relative to spontaneous activity (0 to 20 times average spontaneous activity).

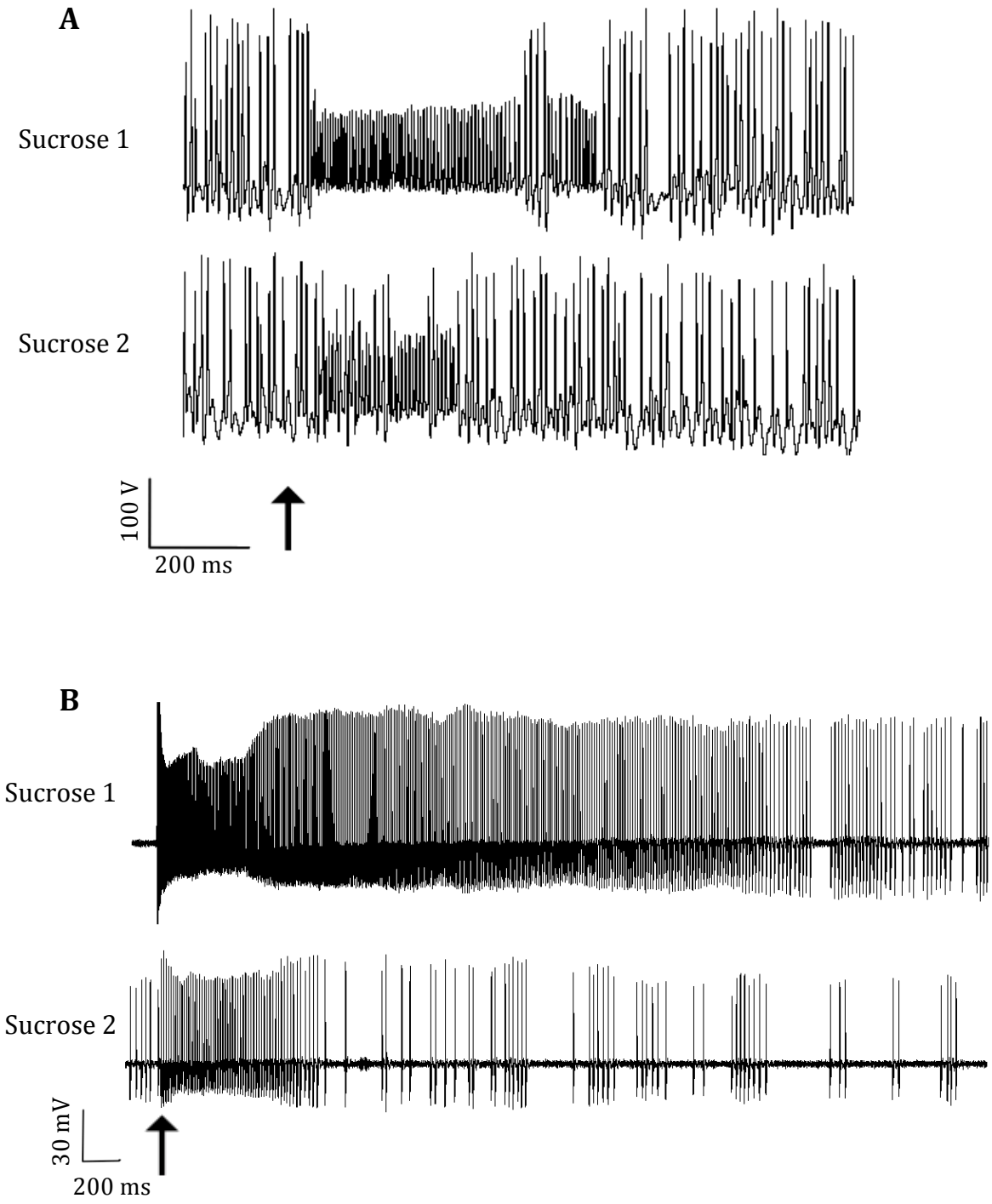

Figure 11. Spike trains from to protocerebral neurons in response to two repetitions of a sucrose stimulus. (A) Spike trains from GN 26 stimulated at the left antenna. (B) Spike trains from GN 25 stimulated at the right antenna. Sucrose 1 and Sucrose 2 are the spike trains in response to the first and second stimulation with sucrose, respectively. Note that in both neurons the first stimulation produces a response of higher spiking frequency and longer duration. The arrow indicates stimuli onset.

3.2 Morphology of protocerebral GNs

The organization of protocerebral GNs into three separate classes is based on physiological characteristics. The stained neurons belonging to each group did not display any common morphological features that supported the particular classification. Nonetheless, the stained neurons are presented according to the group-wise organization.

Three neurons belonging to class 1 GNs (GN 1, 6 and 9) were successfully stained, representing neurons with different morphology. Because of limited time, only GN 1 was reconstructed. This neuron, excited by sucrose application to the proboscis, showed a bilateral morphology with dendrites and soma situated in the right brain hemisphere and axonal projections in the contralateral hemisphere (Fig 12: A, B, C). The soma was located in the outer cell body layer laterally in the SOG. Two dendritic branches extended into the SOG, and others in parallel with the ascending axon, innervating the AMMC (Fig 12: D, E, F). The axon ran close to the esophagus on the ipsilateral side, before crossing the midline just dorsal to the esophagus and ventral to the central body (CB). The axonal projection bifurcated, branching in posterior and anterior direction. An anterior branch projected close to the left AL, and a posterior branch ventrally to the lobes and peduncle of the left mushroom body (Fig 12: G, H, I). GN 6, excited by sucrose stimulation of the right antenna, had its soma located in the perikaryon layer of the right ventral lateral protocerebrum and neuronal processes positioned dorsally to the cell body and medially to the optic lobes (OLs). One branch extended into the right OLs, bifurcated and ramified in parallel in the lobula complex. A confocal image of GN 6 is presented in appendix III (Fig. 16). GN 9, excited by NaCl stimulation of the left antenna, was confined to the protocerebral neuropile. It resided mainly dorsomedially to dorsolaterally in the left protocerebrum, showing prominent projections in this area. A bilateral projection was also visible, crossing the midline proximal to the CB. The soma could not be identified, probably due to damage caused by the insertion of the microelectrode. A confocal image of GN 9 is shown in appendix III (Fig. 17).

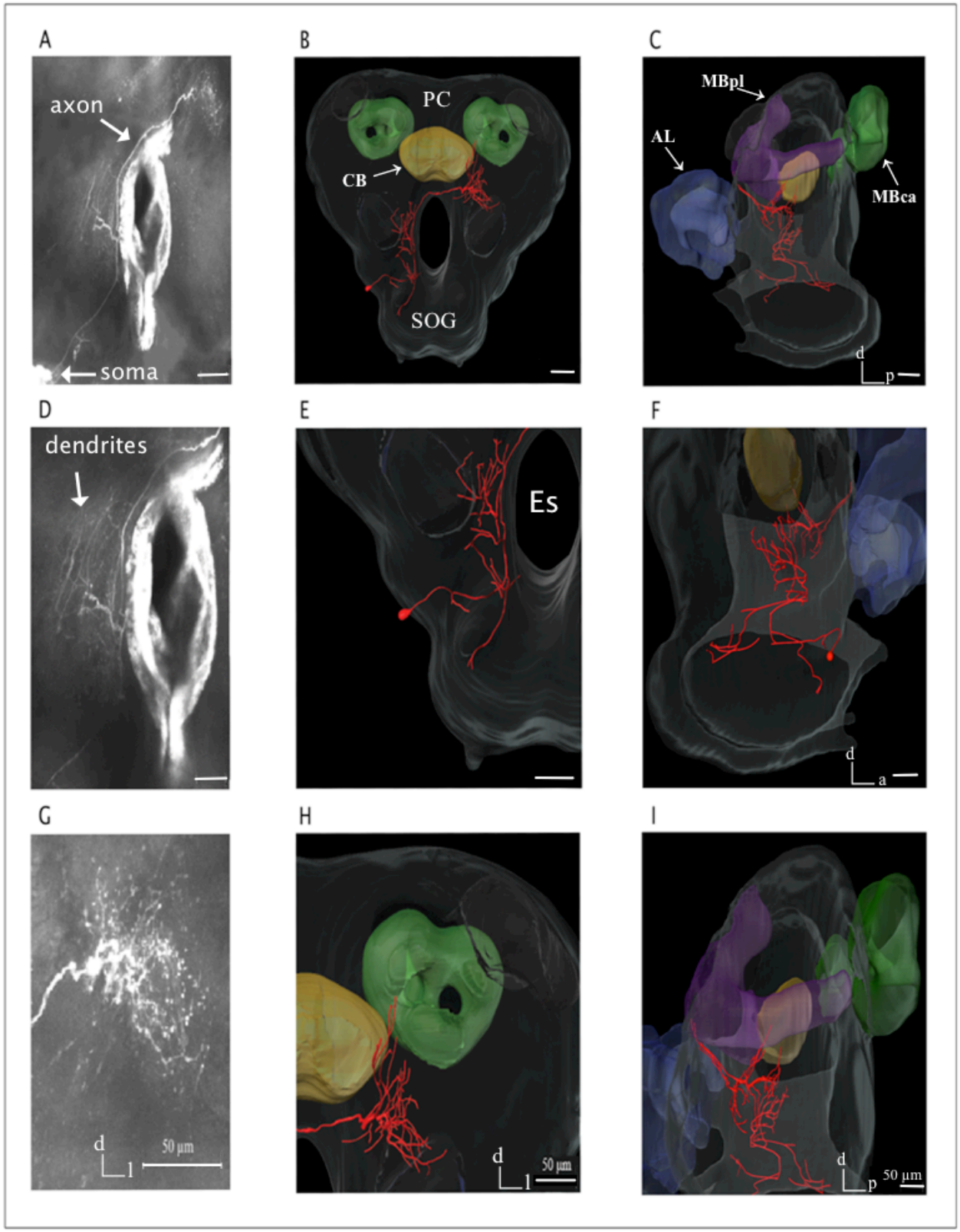

Figure 12. Morphology of GN 1 shown by confocal images and 3D-reconstructions. Left column shows confocal images, while middle and right column show 3D-reconstructions of GN 1 included in the SBA. Top row displays overview photos of GN 1 in frontal (A, B) and lateral orientation (C). Middle row displays close-up photos of the dendrites in frontal (D, E) and lateral (F) orientation. Bottom row displays close-up photos of the axonal projections in frontal (G, H) and lateral (I) orientation. Subesophageal Ganglion (SOG). Protocerebrum (PC). Central Body (CB). Antennal Lobe (AL). Mushroom Body calyces (MBca). Mushroom Body peduncle and lobes (MBpl). Esophagus (Es).

Two neurons, GN 17 and GN 19, belonging to class 2 GNs were successfully stained. GN 17, inhibited by sucrose and quinine and excited by tactile stimulation of the left antenna, resided in the left brain hemisphere. Its cell body was located in the left SOG, and branches were present in the SOG (Fig. 13: A, C), in the ventral protocerebrum, and the AMMC of the deutocerebrum (Fig. 13: A, B). Axonal collaterals (blebs) were present in the SOG and possibly the protocerebrum. GN 19, responding by inhibition to the three gustatory stimuli applied to the left antenna, innervated both primary olfactory centers: the ALs. Extensive branching was present in the majority of glomeruli in the left AL and a soma was recognizable in the lateral cell cluster of the right AL (appendix III, Fig. 18: A). However, it was difficult to trace a neurite to the soma. Furthermore, the neuron had arborizations in the left and right lateral protocerebrum and the left mushroom body calyces (MBca) (appendix III, Fig. 18: B, C, D).

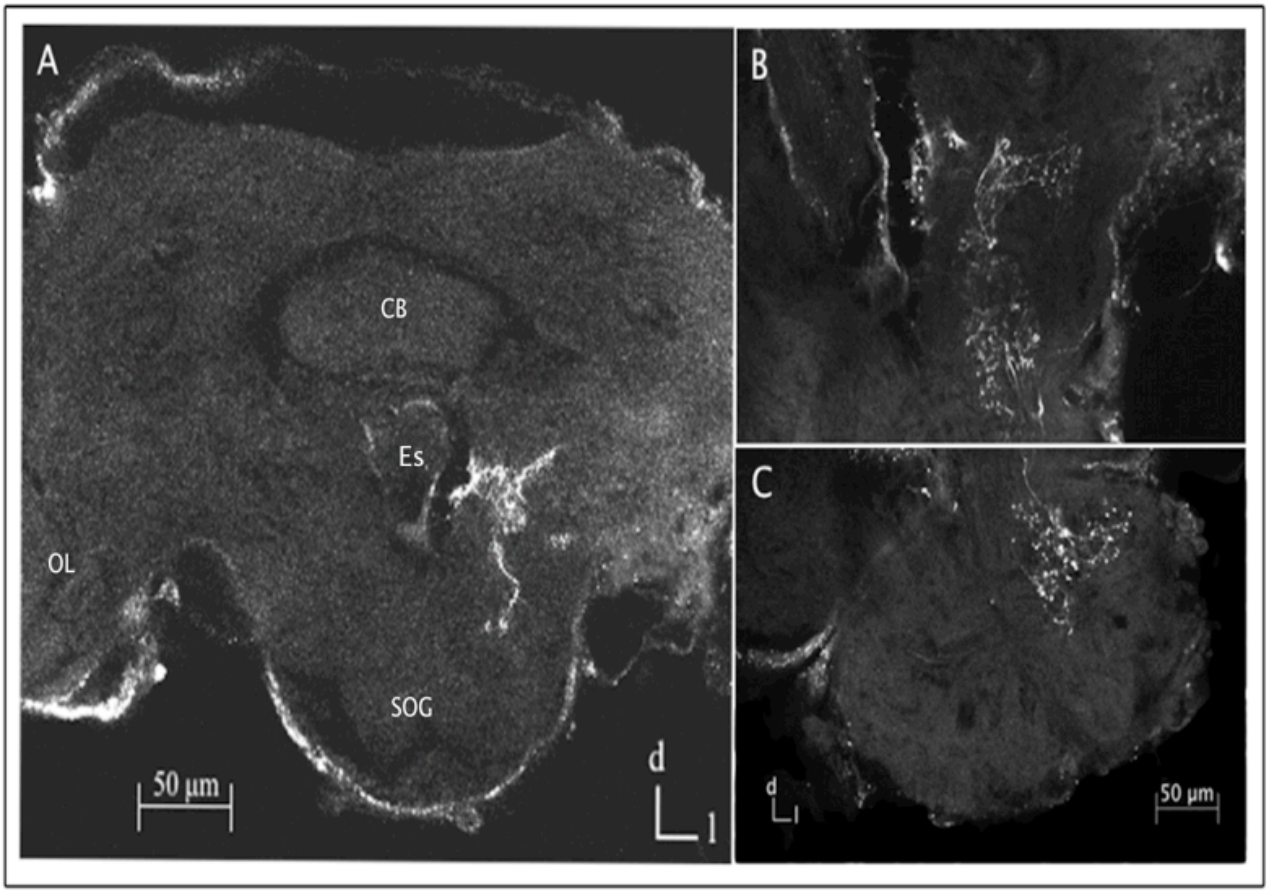

Figure 13. Confocal images of GN 17. All images are in the frontal plane. (A) Overview of the brain preparation with the stained GN 17. (B) Close-up photo of the arborizations in the left SOG and deutocerebrum. (C) Close-up photo of the projections in the left SOG.

Three neurons belonging to class 3 GNs were stained (GN 22, 23 and 26). GN 22, responding by inhibition to the three tastants applied to the right antenna and quinine applied to the left antenna, had its cell body located in the perikaryon layer of the left ventral medial protocerebrum. The neuron innervated the CB and adjacent areas. Due to the lack of blebs and the proximity to the soma, these arborizations were considered dendritic. Its axon crossed the midline and branched extensively in the right SOG/tritocerebrum. Axonal projections were also present in the right OLs. A confocal image of GN 22 is presented in appendix III (Fig. 19). GN 23, excited by sucrose stimulation of the right antenna and quinine stimulation of the proboscis, was co-stained with two additional neurons (Fig. 14: A). Two of the three neurons had their cell bodies situated in the right protocerebrum, medial to the OLs (Fig. 14: B). Their axons crossed the midline and arborized in the left ventral lateral protocerebrum. The soma of the third neuron was situated in the cell body layer of the left lobula complex (Fig. 14: C). The axon of this neuron crossed the midline and arborized in a manner similar to the other two neurons. Distinct axonal collaterals were present in the right ventral lateral protocerebrum, demonstrating the output area of the third neuron. Furthermore, one branch projected posterior in the medial protocerebrum in both hemispheres, possibly representing the dendritic areas of these neurons. Similar to GN 23, GN 26 was a bilateral neuron, innervating both the left and right protocerebrum. In this brain preparation, several neurons were stained. Nonetheless, one neuron was most clearly stained and was thus considered the neuron in which the intracellular recording took place (GN 26). This neuron, excited by the three tastants applied to the left antenna and the proboscis, had its cell body situated in the dorsal medial cell body layer of the right protocerebrum and dendrites extending ventrally in the right protocerebrum. The axon projected into the left protocerebrum, arborizing extensively. A confocal image of GN 26 is presented in appendix III (Fig. 20).

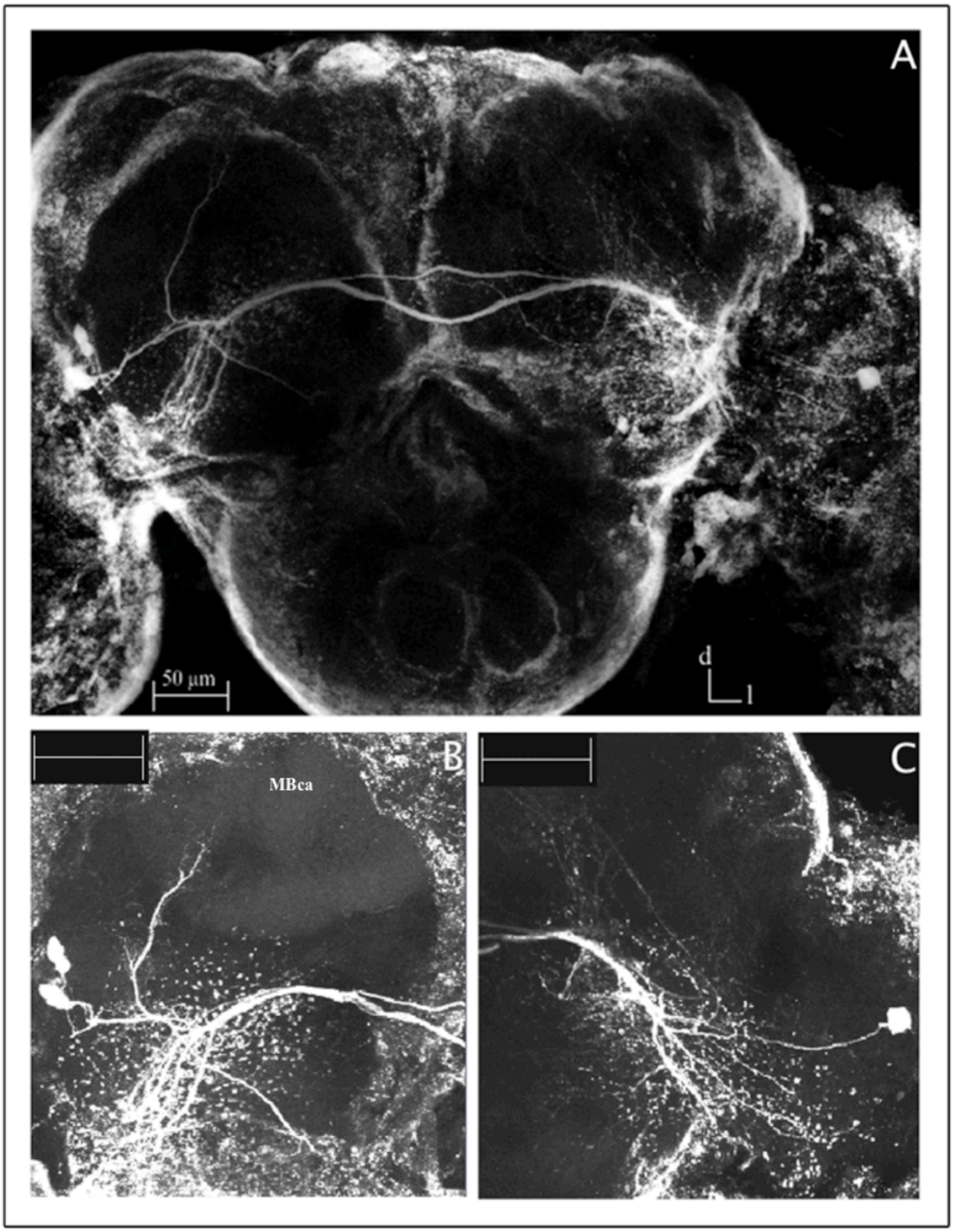

Figure 14. Confocal images of three neurons, GN 23 included, shown in the frontal plane. (A) Overview photo of the three neurons. (B) Close-up photo of the right hemisphere with the two cell bodies and neuronal branching. (C) Close up photo of the left hemisphere with the single cell body and neuronal branching. Scale bars = 50 µm.

4 Discussion

The data from the present study have been gathered as part of a larger project, aiming at understanding the neural circuit processing of gustatory information in the tobacco budworm moth *H. virescens*. Intracellular recordings from protocerebral neurons, combined with fluorescent staining, were carried out in this study. The results provided information about the neuronal morphology and physiology, including how the neurons responded to stimulation with different taste qualities applied to different appendages. The neurons showed large variation in the morphology and the physiological response profiles, some neurons responding more selectively to different modalities and application sites than others. When stimulating with different modalities, individual broadly tuned GNs generally displayed differences in response strengths, as well as different response frequency distributions. In the results section, the physiology and morphology of the protocerebral GNs are presented separately and the discussion will follow the same outline.

4.1 Comparison between the response properties of protocerebral and SOG GNs

To understand how gustatory information is processed and how tastants elicit taste-related behaviors, it is important to comprehend how taste information is handled at every synaptic step. In a previous study of *H. virescens*, the response properties of the GRNs and their axonal projections in the primary taste center (SOG) have been described, providing knowledge about the detection of taste qualities and how this information is relayed to the SOG (Jørgensen *et al.*, 2006; Jørgensen *et al.*, 2007a). Furthermore, intracellular recordings have shown that neurons in the SOG integrate different gustatory information mediated by different appendages (Kvello *et al.*, 2010). In the present study, the analyses of the 26 protocerebral GNs revealed differences between the protocerebral and the SOG neurons. An observable difference was evident by looking at their spontaneous activities. The majority of the SOG neurons exhibited no or low spontaneous activity (0-20 Hz) (Kvello *et al.*, 2010). In contrast, the protocerebral neurons, with one exception, displayed spontaneous spiking activity. Half of the population of recorded protocerebral GNs, categorized as class 1 GNs, displayed spontaneous activity between 0-20 Hz, whereas the remaining 13 neurons exhibited spontaneous activity between 18-70 Hz. Thus, the protocerebral neurons in general displayed higher spontaneous activity than the SOG neurons.

A notable difference between the response properties of SOG and protocerebral neurons was that the majority of the 26 protocerebral GNs showed higher response specificity, responding to stimulation of one appendage only. These were classified as class 1 GNs, responding specifically to one tastant, and class 2 GNs, responding to several stimuli. In contrast to the appendage specificity observed in class 1 and 2 GNs, the majority of GNs in the SOG responded to stimulation of several appendages (Kvello *et al.*, 2010). Moreover, they frequently responded to several modalities, differing from the taste quality specificity seen in the protocerebral class 1 GNs. Similarities to the SOG neurons were observed in the protocerebral class 3 GNs, responding to several stimuli applied at several appendages. Although similar in their overall response patterns, class 3 GNs generally showed higher response specificities. Whereas the majority of the SOG GNs responded to stimuli applied to three or four appendages, class 3 GNs, with one exception, responded to stimuli applied to two appendages (Fig. 1: C). Moreover, SOG GNs readily responded to stimulation of both the left and the right antenna. In contrast, only two of the recorded protocerebral neurons responded to stimulation of both antennae, and only by inhibition. Several of the SOG GNs also responded to the same taste modality applied at all tested appendages (Kvello *et al.*, 2010). In this study, only GN 21 showed equivalent characteristics, responding to sucrose stimulation of both antennae and the proboscis. It should be noted that Kvello and colleagues (2010) tested four appendages, whereas only three were used in the present study. Nonetheless, the results from the protocerebrum are comparable to those from the SOG, considering that stimulation of the tarsus yielded relatively few responses in the SOG neurons. In essence, the comparison between protocerebral and SOG GNs led to the assumption that individual protocerebral neurons generally receive more specific gustatory and mechanosensory input than their SOG counterparts. This notion is supported by the correlation analysis, showing more pronounced correlations between responses to stimulation of a single appendage (principally the left antenna), with non-significant relationships across appendages. Hence, the majority of individual protocerebral GNs seem to receive input from a single appendage, with varying degrees of integration between modalities. The highest number of significant response strength correlations was observed for stimulation of the left antenna, suggesting that neurons receiving input from this appendage respond similarly to stimulation of different tastants. The intracellular recordings were carried out from the left brain hemisphere, which may be the reason for the higher number of response correlations observed for stimulation of the left antenna, compared to the proboscis and the right antenna.

The response profiles of the protocerebral GNs have provided an answer to the primary hypothesis in this study, stating that protocerebral GNs receive information about several taste qualities and from several appendages. Among the 26 GNs, only the six class 3 neurons had response properties in accordance with this hypothesis. The 13 class 1 GNs responded to a single tastant applied at a single appendage, thus challenging the hypothesis regarding integration between appendages and between modalities. Furthermore, the seven class 2 GNs responded to several stimuli applied at a single appendage, thus supporting the hypothesis regarding integration between modalities, but arguing against integration between appendages. From the response properties of the class 1, 2 and 3 GNs, it is obvious that the protocerebral GNs display larger variation in their response profiles than what was initially hypothesized.

4.2 Coding in the protocerebrum

Whether protocerebral GNs with similar physiological properties are present in other insect species is unknown. However, central processing of taste information has been extensively studied in mammals. Although having evolved independently, it is interesting to compare the gustatory systems of mammals and insects. In mammals, coding of gustatory information is transmitted by LL from the periphery to the first relay station in the medulla, the nucleus of the solitary tract (NST) (Spector and Travers, 2005; Carleton *et al.*, 2010). This is equivalent to the LL scheme proposed for GRNs in insects (Wang *et al.*, 2004; Marella *et al.*, 2006). Similar to the SOG GNs described by Kvello and coworkers (2010), mammalian NST GNs displayed varying response tuning breadth, some more selective than others, but all generally more broadly tuned compared to the peripheral afferent fibers (Spector and Travers, 2005; Carleton *et al.*, 2010). Stimulation with sweet, bitter, umami and salt elicited activity in discrete clusters of neurons in the primary gustatory cortex. This means that a cluster responding to a particular taste quality was spatially non-overlapping with clusters activated by other taste qualities, producing a gustotopic map. Furthermore, interspersed between the taste quality hot spots were areas believed to contain broadly tuned neurons (Chen *et al.*, 2011). These findings are analogous with the present results from the protocerebrum of *H. virescens*, showing coexistence of taste quality specific neurons and more broadly tuned neurons. However, one important difference exists regarding gustatory coding in mammals and insects. In contrast to insects, mammals have their taste organs restricted to the oral cavity, presumably making coding of tastant location unnecessary.

Individual GNs in the mammalian central gustatory system, showing varying tuning breadths, have been hypothesized to serve different functions. Narrowly tuned neurons are believed to code taste quality, whereas neurons with broader tuning might execute functions that require less taste discrimination (Spector and Travers, 2005). Although simplistic, this idea is intriguing and may apply to the present results in *H. virescen*s. The discovery of protocerebral GNs with varying tuning breadth indicates coexistence of LL and AFP coding in the protocerebrum. Hypothetically, the narrowly tuned class 1 GNs could act to unequivocally inform the animal about the location and the quality of the taste stimuli. This LL organization would efficiently and reliably inform about the nutritional value and the exact location of the food source or oviposition site. By looking into the response profiles of class 1 GNs (Fig. 1: A), further support is provided for an LL organization in the protocerebrum. From the recorded class 1 GNs, responses to all modalities were obtained. Furthermore, the responses were evoked by stimulating the proboscis and the right antenna with sucrose, the proboscis and antennae with quinine, and the left antenna with NaCl. Thus, the response profiles indicate that each appendage and modality is represented in such a proposed LL mechanism. The diversity in response strengths observed among the class 1 GNs (Fig. 5) implies additional support for an LL mechanism. The differences in response strengths might indicate that information about concentration is processed, where one LL circuit responds with varying strengths to varying concentrations of the preferred stimulus. However, altering the concentrations of the same stimulus was not performed in this study, which was needed to investigate this issue directly. In addition to GNs, neurons that showed no discernible differences in their responses to mechanosensory and gustatory stimuli were found (data not shown). These were regarded as purely mechanosensory and might participate in an LL of this modality.

The more broadly tuned class 2 GNs might provide less information about tastant identity, but be involved in signaling the exact location of the food source, whereas class 3 GNs might participate in an AFP code of taste quality and location. Among the class 2 and 3 GNs, those receiving concomitant mechanosensory and gustatory information might be involved in processing information about the physical aspects of the food source. Physical features, like texture and epicuticular wax composition, have previously been shown to be important elements to the decision of whether to initiate feeding (Powell *et al.*, 1999). The responses of protocerebral GNs to mechanosensory stimulation were usually of opposite mode to their taste responses (Fig. 1: B, C), implying that the protocerebral GNs handle mechanosensory information in a separate manner from gustatory information. Based on the differences in

response strength between taste-evoked responses observed in the majority of class 2 and 3 neurons (Fig. 6 and 7), it is likely that these neurons participate in a discriminatory process of taste quality and location, possibly through an AFP organization.

4.3 Discrimination of stimuli by class 2 and 3 GNs

Four of the seven neurons belonging to class 2 GNs were classified as sucrose-best neurons, responding stronger to sucrose compared to quinine and salt. Three responded by inhibition (GN 17, 19 and 20), possibly mediating aversion, whereas one (GN 14) responded by excitation, possibly mediating acceptance behavior. The existence of protocerebral modality-best neurons is similar to findings of modality-best neurons in the SOG of *H. virescens* and in the mammalian central gustatory system (Spector and Travers, 2005; Carleton *et al.*, 2010; Kvello *et al.*, 2010). In addition, three of the four sucrose-best protocerebral neurons responded to stimulation of either the left or right antenna, suggesting a role also in food orientation behavior. The three remaining class 2 neurons (GN 15, 16, 18) did not display differences in their response strengths, and may thus be candidates to participate in actions requiring little taste discrimination. Moreover, these neurons might be involved in orientation towards the food source, since GN 15 and GN 16 responded to stimulation of the left antenna, and GN 18 to stimulation of the right antenna.

Regarding class 3 GNs, differences in response strengths might be ascribed to a particular taste quality or application site (appendage). GNs that responded strongest to a single modality were regarded as modality-best neurons. Neurons responding strongest to one or two appendages, but with no conspicuous differences between modalities (as decided by the pooled standard deviation estimate), were regarded as appendage-best neurons. Among the six class 3 GNs (Fig. 7), only GN 22, showing strongest inhibition to sucrose stimulation of the right antenna, could with certainty be classified as a modality-best neuron. This neuron also responded by inhibition to quinine and NaCl stimulation of the right antenna, and quinine stimulation of the left antenna. The responses of GN 22 might suggest an involvement of this neuron in inhibiting proboscis extension. In contrast, GN 21 was considered an appendage-best neuron, responding strongest by inhibition to tastant application to both the left and the right antenna, and with weaker inhibition or excitation to tastant application to the proboscis. The strong inhibition in response to all tastants tested at the antennae, combined with excitation in response to quinine application to the proboscis, strongly suggest a role for GN 21 in inhibiting proboscis extension. Another neuron classified as appendage-best was GN 24, responding with a strong excitation to

sucrose stimulation of the right antenna and weaker excitation to sucrose stimulation of the proboscis, whereas stimulation of the left antenna evoked no response. This response profile suggests an involvement in mediating proboscis extension, as well as orientation towards the food source. The remaining class 3 neurons (GN 23, 25, 26) could not be defined as either modality-best or appendage-best neurons. For instance, GN 23 responded with a stronger excitation to sucrose applied to the right antenna than quinine applied to the proboscis, but it did not respond to sucrose application to the proboscis or quinine to the right antenna. Rather than being strictly modality-best or appendage-best, GN 23 is presumably a combination, responding most vigorously when sucrose is applied precisely at the right antenna. In addition, GN 23, 24 and 26 responded to stimuli applied at two appendages, indicating a role in food orientation behavior.

The ultimate function of the gustatory system is to distinguish nutrients from toxic items, hence coding of hedonic values might be important and might be ascribed to class 2 and 3 neurons. The hedonic value coding scheme implies that tastants eliciting similar behaviors are encoded together, in contrast to the encoding of separate taste modalities (de Brito Sanchez, 2011). The phagostimulants sugar, water and low concentrations of salt might be encoded together, all inducing acceptance behavior. Similarly, stimuli inducing avoidance behavior, like bitter compounds and high concentrations of salt, might be encoded together (Yarmolinsky *et al.*, 2009). In mammals, responses of identical modes to the phagostimulant sucrose and the deterrent quinine have not been found, even in the most broadly tuned brainstem neurons (Spector and Travers, 2005). This is in contrast to what is observed in insects. In the metathoracic ganglion of the locust *Schistocerca gregaria* (Rogers and Newland, 2002), in the SOG of the moth *H. virescens* (Kvello *et al.*, 2010) as well as the protocerebral GNs found in this study, several of the GNs responded to both phagostimulants and deterrents. Kvello and coworkers (2010) connected the complex responses of individual SOG GNs to appendage specific behaviors, interpreting the neuronal responses in light of phagostimulatory and aversive behaviors. For instance, neurons excited by the phagostimulants sucrose and water applied to the antennae might participate in eliciting proboscis extension. In the same way, neurons excited by the deterrent quinine applied to the antennae might be involved in inhibiting proboscis extension. This approach was successfully applied to some of the protocerebral neurons in this study, as shown for the four sucrose-best class 2 neurons (GN 14, 17, 19 and 20) and the three class 3 neurons (GN 21, 22 and 24) described in the previous paragraph. Such interpretations are corroborated by behavioral studies in *H. virescens*, demonstrating that sucrose elicits acceptance

behavior, whereas quinine induces aversion (Ramaswamy, 1987b; Ramaswamy *et al.*, 1992; Jørgensen *et al.*, 2007b). Moreover, salts have been argued to mediate aversion (Dethier, 1973; Dethier, 1977). In fact, it has been reported that NaCl at concentrations above 0.1 M (the concentration used in the present study) inhibit feeding in lepidopteran species (Bernays and Chapman, 2001b). The processing of these compounds in a hedonic value arrangement is further supported by a study of the metathoracic ganglion in the locust *S. gregaria*. In that study, Rogers and Newland (2002) discovered that the response duration of spiking local interneurons was dependent on both stimulus identity and concentration. Moreover, stimuli producing similar behavior elicited responses with similar duration. For instance, consistently stronger responses were observed to the deterrents NaCl (0.25 M) and nicotine hydrogen tartrate (0.005 M) compared to the phagostimulants water and sucrose (0.25 M). This observation led the authors to suggest that the behavioral effectiveness (i.e. hedonic value) is encoded, rather than the distinct modalities.

In the wild, insects encounter food sources consisting of complex taste mixtures. Hence, a neural circuit in the brain suited to process complex taste information may be present. Class 2 and 3 neurons, showing varying response sensitivity to stimulation with different modalities, might operate in a population code dealing with discrimination and processing of complex taste mixtures. Unfortunately, mixtures of tastants have not been applied as stimuli in the study of the SOG neurons or the protocerebral neurons in the present study. However, tastant interactions have been investigated in the peripheral gustatory system of *H. virescens*. It was showed that sucrose- and water-responsive GRNs located on the antennae and sucrose-responsive GRNs on the ovipositor were inhibited by alkaloids, indicating taste mixture interactions (Ramaswamy *et al.*, 1992; Jørgensen *et al.*, 2007a). Electrophysiological recordings from two other lepidopteran species, the butterfly *Pieris napi* and the caterpillar of the tiger moth *Grammia geneura,* showed that individual GRNs responded differently when stimulated with binary or complex mixtures compared to single compounds (van Loon, 1996; Bernays and Chapman, 2001a). Moreover, behavioral studies in humans have indicated that a constituent in a taste mixture is usually perceived as less salient compared to stimulation with the component alone. This is thought to arise due to neural processing and not to chemical interactions in the mixture (Lawless, 1979). A neural circuit in the central gustatory system devoted to the processing of taste mixtures has not yet been identified. However, the broadly tuned neurons found in the mammalian primary gustatory cortex has been suggested to participate in such a system (Chen *et al.*, 2011). To understand how single protocerebral neurons are involved in the processing of taste mixtures,

more detailed studies using taste mixtures and their single constituents at different concentrations are needed.

Traditionally, neurons participating in LL or AFP mechanism have been considered to mediate taste information by rate coding, i.e. conveying information by the average neuronal firing rate. However, by only looking at the average firing rate, vital information present in the temporal expression of the response might be lost. Temporal codes in form of spike timing, spike discharge patterns and spike synchronicity are receiving increased attention by gustatory neurophysiologists, as well as researchers working with other sensory systems. Thus, responses of the GNs in the present study were analyzed to find out if temporal patterns may be used to discriminate different stimuli. The FFT procedure used in this study is commonly used to analyze EEG recordings, but is also applicable to spike trains from single cell recordings (Koch and Segev, 1998; Windhorst and Johansson, 1999). Emerging from this analysis was clear differences in temporal expression between responses elicited by different stimuli, exemplified by GN 26 (Fig. 8 and 9). However, the differences in firing frequency distribution between two repetitions of the same stimulus were prominent (Fig. 10). Because of the variability observed in responses elicited by the same stimulus, it was difficult to infer whether class 2 and 3 neurons utilized spike discharge patterns to distinguish between different stimuli. Only two repetitions of each stimulus were conducted in this study, thus it cannot be excluded that stimulus specific temporal features could have emerged with more extensive testing, e.g. a sucrose specific temporal pattern distinct from that of quinine. Another interesting occurrence was that the first stimulation with a modality generally yielded a response of hiher firing frequency than the subsequent stimulation, as exemplified by the responses to sucrose stimulation mediated by the left antenna in GN 26 and the right antenna in GN 25 (Fig. 11). Since these stimulations were not conducted in succession, but instead interspersed between stimulation with other modalities, the difference is presumably not a result of sensory adaptation. Although it is difficult to assess, this pattern might be a means of neuronal communication. As indicated by the spike frequency analysis, the protocerebral GNs do not seem to rely on specific temporal spike discharge patterns to distinguish stimuli. However, this type of coding is shown to be important in the caterpillar of the tobacco hornworm *Manduca sexta*. It was concluded that this species is able to discriminate compounds detected by the same bitter-sensitive receptor neurons, as long as these compounds elicit responses with distinct spike discharge patterns (Glendinning *et al.*, 2006). In addition, temporal coding has been thoroughly investigated in mammals, where it is believed to have a

functional significance. However, the exact information value carried by specific temporal patterns has been difficult to determine (Hallock and Di Lorenzo, 2006).

The second hypothesis in this study states that broadly tuned neurons participate in a discriminatory process of stimuli, by displaying differences in their average response strength and temporal pattern to different stimuli. The present results showed that neurons generally respond to different stimuli with different average strengths, thus these differences may have a functional significance. In contrast, the results did not show any consistent pattern indicating that temporal coding in form of spike discharge patterns occurs in protocerebral GNs. Hence, the second hypothesis seems to be in line with the results regarding discrimination by average response strength, but not by temporal patterns. One possibility might be that temporal codes are more important to discriminate different compounds within a modality, as shown by Glendinning and coworkers (2006), whereas average strength is used to discriminate between gustatory modalities.

The intracellular recording technique is very precise and allows to accurately monitor the activity of a single neuron. However, stable contact between the microelectrode and the interior of the cell is usually intact for only a limited amount of time. These short-lived recordings did not permit stimulating the animal with many modalities applied at many appendages, as well as testing each modality at various concentrations. In the present study, the test substances were sucrose (1.0 M), NaCl (0.1 M) and quinine (0.01 M). Since the modalities were presented at unequal concentrations, the differences in the response strengths and temporal patterns observed in protocerebral class 2 and 3 GNs might be due to stimulation with different concentrations, rather than resulting from stimulation with different modalities. In fact, one drawback of the AFP theory is the difficulty of distinguishing a preferable taste quality at low intensity from an unfavorable one at high intensity (Spector and Travers, 2005). For instance, a neuron displaying higher sensitivity to sucrose than quinine will respond in a similar manner to low concentrations of sucrose and high concentrations of quinine. The importance of concentration to taste perception has been shown in *Drosophila*, where a behavioral assay has been utilized to investigate discrimination of compounds within a modality. In this taste associative learning paradigm, heat was paired with the presentation of fructose, which resulted in the flies displaying learned avoidance to this compound. Importantly, the flies showed aversion to lower, but not higher concentrations of fructose. By using different concentrations of fructose and glucose, the flies were able to differentiate between the compounds. However, their different chemical

identities did not seem to be important factors in the discrimination process. These results indicated discrimination based on palatability, brought about by concentration rather than differences in chemical identity (Masek and Scott, 2010).

4.4 Morphology of protocerebral GNs

By connecting the morphology of the protocerebral GNs to their physiological properties, the ultimate goal is to obtain a coherent image of the overall function of the GNs and how they might establish synaptic connections in the gustatory neural network. In this study, eight neurons were successfully stained. The morphology of these stained confirmed that they were protocerebral neurons, since all were partially or entirely located in the protocerebrum.

Compared to the SOG neurons described by Kvello and coworkers (2010), the protocerebral GNs generally displayed increased response specificities. This feature of the protocerebral GNs might arise by these neurons receiving selective input from modality-best SOG projection neurons or from SOG projection neurons tuned to a specific modality. The staining of GN 1, a neuron projecting from the SOG to the protocerebrum, provided information about this issue. This neuron had dendrites located in the right SOG and the AMMC, and an axon projecting to the contralateral protocerebral hemisphere in close proximity to the CB (Fig. 12). GN 1 responded specifically to sucrose applied to the proboscis, thus pointing to an increased specificity already in the neural trajectory from the SOG to the protocerebrum. This narrowly tuned neuron might receive its input from narrowly tuned SOG neurons. Some of the SOG GNs responded with the strongest excitation to sucrose applied to the proboscis, with weaker excitation or no response to stimulation with other modalities applied to the proboscis, tarsus and antennae (Kvello *et al.*, 2009; Kvello *et al.*, 2010). Thus, these neurons are good candidates to feed information onto GN 1. Another neuron innervating the SOG, the protocerebrum and the AMMC of the deutocerebrum was GN 17 (Fig. 13). This neuron responded to stimuli applied to the left antenna: by inhibition to stimulation of sucrose and quinine, and by excitation to tactile stimulation. It was difficult from the morphology to clearly determine whether the branches located in the AMMC and the protocerebrum were pre- or postsynaptic. A previous study presented results showing that mechanosensory fibers from the antennae project mostly to the ipsilateral AMMC, but also in the SOG. Likewise, fibers assumed to be gustatory were found to project both in the AMMC and the SOG (Jørgensen *et al.*, 2006). The most prominent axon collaterals of GN 17 were present in the SOG, suggesting that this neuron receives gustatory and mechanosensory information in the AMMC and relays it to the SOG and possibly the

protocerebrum. As illustrated in GN 17, uncertainty existed regarding whether neuronal branches were dendritic or axonal. The morphological results provided by the fluorescent staining technique did not provide direct evidence about this issue. This method provided information about the overall neuronal morphology, making it possible to infer the input and output areas based on features like the appearance of blebs. However, caution should be taken when trying to assess the dendritic and axonal terminals of a stained neuron.

An interesting multimodal area in the brain is the lateral protocerebrum, a region shown to receive olfactory, visual and gustatory information (Schröter and Menzel, 2003; Wessnitzer and Webb, 2006; Farris, 2008). This neuropile contains descending olfactory neurons, as shown in *M. sexta* (Kanzaki *et al.*, 1991) and *H. virescens* (Løfaldli, unpublished data), and is considered to be a premotoric area. GN 9, excited by NaCl applied to the left antenna, innervated this area (appendix III, Fig. 17). It had neuronal processes also in the right dorsomedial protocerebrum and dorsomedially to dorsolaterally in the left protocerebrum. However, it was difficult to clearly distinguish the axonal and the dendritic terminals, due to the damage caused by the insertion of the microelectrode. Thus, it was difficult to determine whether the innervation of the lateral protocerebrum is pre- or postsynaptic. Similar to GN 9, GN 23 and GN 26 displayed a bilateral morphology, having dendrites in one hemisphere and axonal projections in the contralateral hemisphere. GN 23 was co-stained with two other neurons, and interestingly, the three neurons showed a remarkably similar morphology (Fig. 14). Two of these neurons had their cell bodies in the right protocerebral hemisphere and axons projecting to the contralateral hemisphere. The third neuron had its cell body in the left protocerebral hemisphere and an axon projecting to the contralateral hemisphere. The neurons had a branch extending posteriorly in both protocerebral hemispheres, possibly representing the dendritic areas. The functional significance of the observed morphological symmetry is not known. However, a tempting idea is that these neurons respond to similar taste modalities, but applied to different appendages. GN 23 responded to sucrose application to the right antenna and quinine application to the proboscis. Thus, the contralateral neuron(s) might respond similarly to stimulation of the left antenna. An interesting feature of GN 26, having dendrites in the right protocerebrum and axonal projections in the left protocerebrum, is that it responded to stimulation of the left antenna and the proboscis, while the morphology indicated information transfer to the left protocerebrum (appendix III, Fig. 20). Thus, information from the GRNs located on the left antenna and proboscis seem to have been relayed to the contralateral hemisphere, before being transferred back to the left hemisphere by GN 26.

GN 1, 9, 17, 23 and 26 are believed to participate directly in the coding of taste quality and location. In contrast, the remaining three stained GNs are hypothesized to have modulatory roles. Two of them connected the gustatory system with the OLs. GN 6, responding by excitation to sucrose applied to the right antenna, innervated the right OLs and had also processes in the right dorsolateral protocerebrum. Although difficult to determine the input and output areas of this neuron, the innervation of the OLs seemed to contain axon collaterals (appendix III, Fig. 16). Thus, information is probably mediated to this area. GN 22 responded by inhibition to the three tastants applied to the right antenna and quinine applied to the left antenna. This neuron, receiving input in the CB and adjacent areas, had axonal projections in the SOG/tritocerebrum and the right OLs (appendix III, Fig. 19). The OLs are substructures of the protocerebrum involved in the processing of visual information from the compound eye (Strausfeld, 1970; Chapman, 1998), while the CB is a higher brain center involved in limb coordination and orientation (Loesel *et al.*, 2002; Heinze and Homberg, 2007). Although *Heliothis* spp. are nocturnal, vision is important for orientation. At dusk or during night, these species use vision to find food, oviposition sites and mating partners (Fitt, 1989; Cutler *et al.*, 1995). Hence, vision, as well as olfaction, seem to be necessary for the initial recognition and approach to a possible food or oviposition site, as shown for vision in the shark moth *C. umbratica* and olfaction in *H. virescens* (Brantjes, 1976; Tingle and Mitchell, 1992). Based on the morphology and physiology of GN 6 and GN 22, a direct neuronal connection between the visual and gustatory systems can be envisaged. Furthermore, an appealing idea is that GNs relaying gustatory information to the OLs might be modulatory, affecting the processing of visual information upon feeding. Unfortunately, neither GN 6 nor GN 22 was tested with visual stimuli. However, several of the other GNs in this study responded to light stimuli (data not shown), further supporting a direct connection between the visual and gustatory system.

Another neuron hypothesized to be modulatory was GN 19. This neuron innervated the left and the right lateral protocerebrum, as well as both ALs and the left MBca, structures previously shown to be important in the processing of olfactory information (Hansson, 1995; Hildebrand, 1996). Overall, the morphology of GN 19 resembled a modulatory serotonin-immunoreactive (SI) neuron characterized in another Heliothine species, the oriental tobacco budworm moth *Helicoverpa assulta* (Zhao and Berg, 2009), and also reported in several other insect species, e.g. the silkmoth *Bombyx mori* and the American cockroach *Periplaneta americana* (Salecker and Distler, 1990; Hill et al., 2002). Due to limited time, double labeling with serotonin immunocytochemistry was not performed, which is needed to confirm whether GN 19 is an SI

neuron. Nonetheless, GN 19 showed similarities to the SI neurons of *B. mori*, *P. americana* and *H. assulta*, all of them innervating the left and right protocerebrum and both ALs. Furthermore, GN 19 and the SI neuron of *B. mori* and *P. americana* innervated the MBca, whereas the SI neuron of *H. assulta* did not. The neuronal processes of GN 19 located in the MBca were thick and blebby (appendix III, Fig 18: D), similar to the axon collaterals observed in *P. americana*, but differing from the fine processes observed in *B. mori* (Salecker and Distler, 1990; Hill *et al.*, 2002). It was difficult to clearly determine whether the neuronal processes of GN 19 in the left AL and the lateral protocerebrum were pre- or postsynaptic (appendix III, Fig. 18: A, B, C). In the SI neuron of *B. mori, P. americana* and *H. assulta,* the neuronal processes in the AL is presynaptic, which is also likely to be the case for GN 19. Therefore, the neuronal arborizations in the lateral protocerebrum are presumably postsynaptic, which is similar to the SI neurons in *B. mori, P. americana* and *H. assulta* (Salecker and Distler, 1990; Hill *et al.*, 2002; Zhao and Berg, 2009). The SI neurons in *B. mori* and *H. assulta* were physiologically characterized, responding with excitation to various odors. In contrast, GN 19 responded with a pronounced inhibition to all tested taste modalities, suggesting an antagonistic role mediated by gustatory stimulation. Regardless of the exact operating mode, GN 19 provides compelling evidence of gustatory interaction in a circuit previously shown to mediate olfactory and mechanosensory information (Hill *et al.*, 2002; Zhao and Berg, 2009).

4.5 Topics for further research

Traditionally, investigations of the insect gustatory system have focused on GRNs, their projections to the central nervous system and the processing of gustatory information in thoracic ganglia and the SOG. The SOG receives massive input from contact chemosensilla and houses motor neurons responsible for movement of the proboscis (Rehder, 1988; Rajashekhar and Singh, 1994; Gordon and Scott, 2009). This organization has led to the belief that gustatory processing in the SOG is sufficient to carry out feeding behavior, which is corroborated by the observation that SOG GNs are in close anatomical proximity to GRN output targets and SOG motor neurons (Kvello *et al.*, 2010). Hence, SOG gustatory interneurons are well positioned to carry out the necessary processing of gustatory information and relay it to motor neurons controlling movement of the mouthparts. However, the results from this study have shown that GNs are represented in many areas of the protocerebrum and that extensive gustatory processing also occurs in this brain region. To develop our understanding of insect gustation, future research should investigate the protocerebral gustatory system in more detail, focusing on both physiological and morphological characteristics of protocerebral GNs. By employing different

concentrations of the same modality and several repetitions of each stimulus, one could investigate more thoroughly the importance of temporal codes to the discrimination of stimuli. Moreover, testing with different sugars and different bitter compounds would provide valuable insight into the neural information processing of different compounds within a modality. By also carrying out behavioral studies using the same compounds, a better connection between the neural processing of these compounds and their importance to taste-related behavior would be obtained. Another interesting topic to explore would be how complex taste mixtures are processed in the brain, whether they are processed separately or in a population code together with the processing of single components. Finally, the understanding of protocerebral gustatory processing could benefit from research mapping the morphology of GNs more thoroughly.

5 Conclusion

The results from this study have demonstrated that GNs innervate many regions of the protocerebrum, including areas like the lateral protocerebrum, the central body and the optic lobes. Moreover, the physiological results showed that the recorded protocerebral GNs display variation in their response tuning breadth to stimulation with mechanosensory and gustatory modalities applied at different appendages. Some protocerebral neurons are narrowly tuned, responding to a single modality applied at a single appendage (class 1 GNs). Others are more broadly tuned, responding to different modalities applied at one, two or three appendages (class 2 and 3 GNs). The majority of the broadly tuned neurons were found to respond differently to stimulation with different taste qualities. The analysis of the responses indicate a discriminatory process of taste qualities by means of average rate coding, but not temporal spike discharge patterns. By responding differently to the various stimuli, the class 2 and 3 GNs meet the requirements to participate in an AFP model, whereas the narrowly tuned class 1 GNs are ideally suited to take part in LL coding. Thus, the results presented in this study argue that the protocerebral gustatory system makes use of both LL and AFP coding in the processing of taste information. Furthermore, the morphological and physiological characteristics indicate a direct role of these neurons in gustatory coding, as well as an involvement of some GNs in modulating the activity of other sensory pathways.

6 Abbreviations

AFP	–	Across Fiber Pattern
AL	–	Antennal Lobe
AMMC	–	Antennal Mechanosensory and Motor Center
CB	–	Central Body
CLSM	–	Confocal Laser-Scanning Microscope
Es	–	Esophagus
FFT	–	Fast Fourier Transform
GN	–	Gustatory Neuron
GRN	–	Gustatory Receptor Neuron
LL	–	Labelled Line
LP	–	Lateral Protocerebrum
MBca	–	Mushroom Body calyces
MBpl	–	Mushroom Body peduncle and lobes
NGS	–	Normal Goat Serum
NST	–	Nucleus of the Solitary Tract
OL	–	Optic Lobe
PBS	–	Phosphate Buffered Saline
PBStx	-	Phosphate Buffered Saline with triton x
PC	–	Protocerebrum
SBA	–	Standard Brain Atlas
SOG	–	Subesophageal Ganglion

7 References

Amrein, H. and Thorne, N. (2005), Gustatory perception and behavior in *Drosophila melanogaster*, *Current Biology,* 15:R673-R684.

Bernays, E. A. and Chapman, R. F. (2001a), Electrophysiological responses of taste cells to nutrient mixtures in the polyphagous caterpillar of *Grammia geneura*, *Journal of Comparative Physiology A-Sensory Neural and Behavioral Physiology,* 187:205-213.

Bernays, E. A. and Chapman, R. F. (2001b), Taste cell responses in the polyphagous arctiid, *Grammia geneura*: towards a general pattern for caterpillars, *Journal of Insect Physiology,* 47:1029-1043.

Bloomfield, P. (2000). *Fourier analysis of time series: an introduction,* 2nd ed., John Wiley & Sons, New York, 288 pp

Boschker, M. (2010). *The tarsal gustatory system in Heliothis virescens: Physiological characterisation and functional tracing of receptor neurones in the prothoracic ganglion.* Master thesis, Norwegian University of Science and Technology.

Brandt, R., Rohlfing, T., Rybak, J., Krofczik, S., Maye, A., Westerhoff, M., Hege, H. C. and Menzel, R. (2005), Three-dimensional average-shape atlas of the honeybee brain and its applications, *Journal of Comparative Neurology,* 492:1-19.

Brantjes, N. (1976), Senses involved in the visiting of flowers by *Cucullia umbratica* (Noctuidae, Lepidoptera), *Entomologia Experimentalis Et Applicata,* 20:1-7.

Bredendiek, N., Hutte, J., Steingraber, A., Hatt, H., Gisselmann, G. and Neuhaus, E. M. (2011), Go alpha is involved in sugar perception in *Drosophila*, *Chemical Senses,* 36:69-81.

Cameron, P., Hiroi, M., Ngai, J. and Scott, K. (2010), The molecular basis for water taste in *Drosophila*, *Nature,* 465:91-95.

Carleton, A., Accolla, R. and Simon, S. A. (2010), Coding in the mammalian gustatory system, *Trends in Neurosciences,* 33:326-34.

Chapman, R. F. (1998). *The insects: structure and function,* 4th ed., Cambridge University Press, Cambridge, 770 pp

Chen, X. K., Gabitto, M., Peng, Y. Q., Ryba, N. J. P. and Zuker, C. S. (2011), A gustotopic map of taste qualities in the mammalian brain, *Science,* 333:1262-1266.

Clyne, P. J., Warr, C. G. and Carlson, J. R. (2000), Candidate taste receptors in *Drosophila*, *Science,* 287:1830-1834.

Cutler, D. E., Bennett, R. R., Stevenson, R. D. and White, R. H. (1995), Feeding-behavior in the nocturnal moth *Manduca sexta* is mediated mainly by blue receptors, but where are they located in the retina, *Journal of Experimental Biology,* 198:1909-1917.

de Brito Sanchez, M. G., Giurfa, M., Mota, T. R. D. and Gauthier, M. (2005), Electrophysiological and behavioural characterization of gustatory responses to antennal 'bitter' taste in honeybees, *European Journal of Neuroscience,* 22:3161-3170.

de Brito Sanchez, M. G. (2011), Taste perception in honey bees, *Chemical Senses,* 36:675-692.

Dethier, V. G. (1955), The physiology and histology of the contact chemoreceptors of the blowfly, *Quarterly Review of Biology,* 30:348-371.

Dethier, V. G. and Hanson, F. E. (1968), Electrophysiological responses of the chemoreceptors of the blowfly to sodium salts of fatty acids, *Proceedings of the National Academy of Sciences of the United States of America,* 60:1296-1303.

Dethier, V. G. (1973), Electrophysiological studies of gustation in Lepidopterous larvae. 2. Taste spectra in relation to food-plant discrimination, *Journal of Comparative Physiology,* 82:103-134.

Dethier, V. G. (1977), The taste of salt, *American Scientist,* 65:744-751.

Dunipace, L., Meister, S., Mcnealy, C. and Amrein, H. (2001), Spatially restricted expression of candidate taste receptors in the *Drosophila* gustatory system, *Current Biology,* 11:822-835.

Edgecomb, R. S. and Murdock, L. L. (1992), Central projections of axons from taste hairs on the labellum and tarsi of the blowfly, *Phormia regina* Meigen, *Journal of Comparative Neurology,* 315:431-444.

Erickson, R. P. (2000), The evolution of neural coding ideas in the chemical senses, *Physiology & behavior,* 69:3-13.

Erickson, R. P. (2008), A study of the science of taste: on the origins and influence of the core ideas, *The Behavioral and brain sciences,* 31:59-105.

Evers, J. F., Schmitt, S., Sibila, M. and Duch, C. (2005), Progress in functional neuroanatomy: precise automatic geometric reconstruction of neuronal morphology from confocal image stacks, *Journal of Neurophysiology,* 93:2331-2342.

Farris, S. M. (2008), Tritocerebral tract input to the insect mushroom bodies, *Arthropod Structure & Development,* 37:492-503.

Fitt, G. P. (1989), The ecology of *Heliothis* species in relation to agroecosystems, *Annual Review of Entomology,* 34:17-52.

Gaffal, K. P. (1979), An ultrastructural study of the tips of four classical bimodal sensilla with one mechanosensitive and several chemosensitive receptor cells, *Zoomorphologie,* 92:273-291.

Glendinning, J. I., Davis, A. and Rai, M. (2006), Temporal coding mediates discrimination of "bitter" taste stimuli by an insect, *Journal of Neuroscience,* 26:8900-8908.

Gordon, M. D. and Scott, K. (2009), Motor control in a *Drosophila* taste circuit, *Neuron,* 61:373-384.

Hallberg, E. (1981), Fine-structural characteristics of the antennal sensilla of *Agrotis segetum* (Insecta: Lepidoptera), *Cell and Tissue Research,* 218:209-218.

Hallock, R. M. and Di Lorenzo, P. M. (2006), Temporal coding in the gustatory system, *Neuroscience and Biobehavioral Reviews,* 30:1145-60.

Hansson, B. S. (1995), Olfaction in Lepidoptera, *Experientia,* 51:1003-1027.

Heinze, S. and Homberg, U. (2007), Maplike representation of celestial e-vector orientations in the brain of an insect, *Science,* 315:995-997.

Hettinger, T. P. and Frank, M. E. (1992), Information processing in mammalian gustatory systems, *Current Opinion in Neurobiology,* 2:469-78.

Hildebrand, J. G. (1996), Olfactory control of behavior in moths: central processing of odor information and the functional significance of olfactory glomeruli, *Journal of Comparative Physiology A - Neuroethology Sensory Neural and Behavioral Physiology,* 178:5-19.

Hill, E. S., Iwano, M., Gatellier, L. and Kanzaki, R. (2002), Morphology and physiology of the serotonin-immunoreactive putative antennal lobe feedback neuron in the male silkmoth *Bombyx mori*, *Chemical Senses,* 27:475-483.

Ignell, R. and Hansson, B. S. (2005), Projection patterns of gustatory neurons in the suboesophageal ganglion and tritocerebrum of mosquitoes, *Journal of Comparative Neurology,* 492:214-233.

Isono, K. and Morita, H. (2010), Molecular and cellular designs of insect taste receptor system, *Frontiers in Cellular Neuroscience,* 4:20.

Jiao, Y., Moon, S. J. and Montell, C. (2007), A *Drosophila* gustatory receptor required for the responses to sucrose, glucose, and maltose identified by mRNA tagging, *Proceedings of the National Academy of Sciences of the United States of America,* 104:14110-14115.

Jiao, Y. C., Moon, S. J., Wang, X. Y., Ren, Q. T. and Montell, C. (2008), Gr64f is required in combination with other gustatory receptors for sugar detection in *Drosophila*, *Current Biology,* 18:1797-1801.

Jørgensen, K., Kvello, P., Almaas, T. J. and Mustaparta, H. (2006), Two closely located areas in the suboesophageal ganglion and the tritocerebrum receive projections of gustatory receptor neurons located on the antennae and the proboscis in the moth *Heliothis virescens*, *Journal of Comparative Neurology,* 496:121-134.

Jørgensen, K., Almaas, T. J., Poll, F. M. and Mustaparta, H. (2007a), Electrophysiological characterization of responses from gustatory receptor neurons of *sensilla chaetica* in the moth *Heliothis virescens*, *Chemical Senses,* 32:863-879.

Jørgensen, K., Stranden, M., Sandoz, J. C., Menzel, R. and Mustaparta, H. (2007b), Effects of two bitter substances on olfactory conditioning in the moth *Heliothis virescens*, *Journal of Experimental Biology,* 210:2563-2573.

Kanzaki, R., Arbas, E. A. and Hildebrand, J. G. (1991), Physiology and morphology of descending neurons in pheromone-processing olfactory pathways in the male moth *Manduca sexta*, *Journal of comparative physiology A - Sensory, neural, and behavioral physiology,* 169:1-14.

Koch, C. and Segev, I. (1998). *Methods in Neuronal Modeling: From Ions to Networks,* 2nd ed., Mit Press, Cambridge, MA, 687 pp

Krieger, J., Raming, K., Dewer, Y. M. E., Bette, S., Conzelmann, S. and Breer, H. (2002), A divergent gene family encoding candidate olfactory receptors of the moth *Heliothis virescens*, *European Journal of Neuroscience,* 16:619-628.

Kvello, P., Almaas, T. J. and Mustaparta, H. (2006), A confined taste area in a lepidopteran brain, *Arthropod Structure & Development,* 35:35-45.

Kvello, P., Løfaldli, B. B., Rybak, J., Menzel, R. and Mustaparta, H. (2009), Digital, three-dimensional average shaped atlas of the *Heliothis virescens* brain with integrated gustatory and olfactory neurons, *Frontiers in systems neuroscience,* 3:14.

Kvello, P., Jørgensen, K. and Mustaparta, H. (2010), Central gustatory neurons integrate taste quality information from four appendages in the moth *Heliothis virescens*, *Journal of Neurophysiology,* 103:2965-2981.

Larsen, J. R. (1962), The fine structure of the labellar chemosensory hairs of the blowfly, *Phormia regina* Meig, *Journal of Insect Physiology,* 8:683-691.

Lawless, H. T. (1979), Evidence for neural inhibition in bittersweet taste mixtures, *Journal of comparative and physiological psychology,* 93:538-47.

Lee, Y., Moon, S. J. and Montell, C. (2009), Multiple gustatory receptors required for the caffeine response in *Drosophila*, *Proceedings of the National Academy of Sciences of the United States of America,* 106:4495-4500.

Liscia, A. and Solari, P. (2000), Bitter taste recognition in the blowfly: Electrophysiological and behavioral evidence, *Physiology & Behavior,* 70:61-65.

Liu, L., Leonard, A. S., Motto, D. G., Feller, M. A., Price, M. P., Johnson, W. A. and Welsh, M. J. (2003), Contribution of *Drosophila* DEG/ENaC genes to salt taste, *Neuron,* 39:133-146.

Loesel, R., Nässel, D. R. and Strausfeld, N. J. (2002), Common design in a unique midline neuropil in the brains of arthropods, *Arthropod Structure & Development,* 31:77-91.

Marella, S., Fischler, W., Kong, P., Asgarian, S., Rueckert, E. and Scott, K. (2006), Imaging taste responses in the fly brain reveals a functional map of taste category and behavior, *Neuron,* 49:285-295.

Masek, P. and Scott, K. (2010), Limited taste discrimination in *Drosophila*, *Proceedings of the National Academy of Sciences of the United States of America,* 107:14833-14838.

McCutchan, M. C. (1969), Responses of tarsal chemoreceptive hairs of the blowfly, *Phormia regina*, *Journal of Insect Physiology,* 15:2059-2068.

Meunier, N., Marion-Poll, F. and Lucas, P. (2009), Water taste transduction pathway is calcium dependent in *Drosophila*, *Chemical Senses,* 34:441-449.

Mitchell, B. K. and Itagaki, H. (1992), Interneurons of the subesophageal ganglion of *Sarcophaga bullata* responding to gustatory and mechanosensory stimuli, *Journal of Comparative Physiology A - Sensory Neural and Behavioral Physiology,* 171:213-230.

Mitchell, B. K., Itagaki, H. and Rivet, M. P. (1999), Peripheral and central structures involved in insect gustation, *Microscopy Research and Technique,* 47:401-415.

Miyazaki, T. and Ito, K. (2010), Neural architecture of the primary gustatory center of *Drosophila melanogaster* visualized with GAL4 and LexA enhancer-trap systems, *Journal of Comparative Neurology,* 518:4147-4181.

Montell, C. (2009), A taste of the *Drosophila* gustatory receptors, *Current Opinion in Neurobiology,* 19:345-353.

Moon, S. J., Lee, Y., Jiao, Y. and Montell, C. (2009), A *Drosophila* gustatory receptor essential for aversive taste and inhibiting male-to-male courtship, *Current Biology,* 19:1623-1627.

Nishino, H., Nishikawa, M., Yokohari, F. and Mizunami, M. (2005), Dual, multilayered somatosensory maps formed by antennal tactile and contact chemosensory afferents in an insect brain, *Journal of Comparative Neurology,* 493:291-308.

Ozaki, M., Takahara, T., Kawahara, Y., Wada-Katsumata, A., Seno, K., Amakawa, T., Yamaoka, R. and Nakamura, T. (2003), Perception of noxious compounds by contact chemoreceptors of the blowfly, *Phormia regina*: putative role of an odorant-binding protein, *Chemical Senses,* 28:349-359.

Pei, S. C. and Tseng, C. C. (1995), Elimination of AC interference in electrocardiogram using IIR notch filter with transient suppression, *IEEE transactions on bio-medical engineering,* 42:1128-32.

Pfaffmann, C. (1959), The afferent code for sensory quality, *American Psychologist,* 14:226-232.

Phillips, C. E. and Vandeberg, J. S. (1976), Mechanism for sensillum fluid-flow in trichogen and tormogen cells of *Phormia regina* (Meigen) (Diptera-Calliphoridae), *International Journal of Insect Morphology & Embryology,* 5:423-431.

Powell, G., Maniar, S. P., Pickett, J. A. and Hardie, J. (1999), Aphid responses to non-host epicuticular lipids, *Entomologia Experimentalis Et Applicata,* 91:115-123.

Press, W. H., Teukolsky, S. A., Vetterling, W. T. and Flannery, B. P. (1992). *Numerical recipes in FORTRAN: the art of scientific computation,* 2nd ed., Cambridge University Press, New York, 963 pp

Rajashekhar, K. P. and Singh, R. N. (1994), Organization of motor-neurons innervating the proboscis musculature in *Drosophila melanogaster* Meigen (Diptera, Drosophilidae), *International Journal of Insect Morphology & Embryology,* 23:225-242.

Ramaswamy, S. B., Ma, W. K. and Baker, G. T. (1987a), Sensory cues and receptors for oviposition by *Heliothis virescens*, *Entomologia Experimentalis Et Applicata,* 43:159-168.

Ramaswamy, S. B. (1987b), Behavioral responses of *Heliothis virescens* (Lepidoptera, Noctuidae) to stimulation with sugars, *Journal of Insect Physiology,* 33:755-760.

Ramaswamy, S. B., Cohen, N. E. and Hanson, F. E. (1992), Deterrence of feeding and oviposition responses of adult *Heliothis virescens* by some compounds bitter-tasting to humans, *Entomologia Experimentalis Et Applicata,* 65:81-93.

Rehder, V. (1988), A neuroanatomical map of the subesophageal and prothoracic ganglia of the honey bee (*Apis mellifera)*, *Proceedings of the Royal Society of London Series B-Biological Sciences,* 235:179-202.

Renwick, J. a. A. and Chew, F. S. (1994), Oviposition behavior in Lepidoptera, *Annual Review of Entomology,* 39:377-400.

Robertson, H. M., Warr, C. G. and Carlson, J. R. (2003), Molecular evolution of the insect chemoreceptor gene superfamily in *Drosophila melanogaster*, *Proceedings of the National Academy of Sciences of the United States of America,* 100:14537-14542.

Robertson, H. M. and Wanner, K. W. (2006), The chemoreceptor superfamily in the honey bee, *Apis mellifera*: expansion of the odorant, but not gustatory, receptor family, *Genome Research,* 16:1395-1403.

Rogers, S. M. and Newland, P. L. (2002), Gustatory processing in thoracic local circuits of locusts, *Journal of Neuroscience,* 22:8324-8333.

Salecker, I. and Distler, P. (1990), Serotonin-immunoreactive neurons in the antennal lobes of the American cockroach *Periplaneta americana*: light- and electron-microscopic observations, *Histochemistry,* 94:463-73.

Sato, K., Tanaka, K. and Touhara, K. (2011), Sugar-regulated cation channel formed by an insect gustatory receptor, *Proceedings of the National Academy of Sciences of the United States of America,* 108:11680-11685.

Schmitt, S., Evers, J. F., Duch, C., Scholz, M. and Obermayer, K. (2004), New methods for the computer-assisted 3-D reconstruction of neurons from confocal image stacks, *Neuroimage,* 23:1283-1298.

Schneider, D. (1964), Insect antennae, *Annual Review of Entomology,* 9:103-122.

Schoonhoven, L. M. (1968), Chemosensory bases of host plant selection, *Annual Review of Entomology,* 13:115-136.

Schröter, U. and Menzel, R. (2003), A new ascending sensory tract to the calyces of the honeybee mushroom body, the subesophageal-calycal tract, *The Journal of comparative neurology,* 465:168-78.

Scott, K., Brady, R., Cravchik, A., Morozov, P., Rzhetsky, A., Zuker, C. and Axel, R. (2001), A chemosensory gene family encoding candidate gustatory and olfactory receptors in *Drosophila*, *Cell,* 104:661-673.

Scott, K. (2005), Taste recognition: food for thought, *Neuron,* 48:455-64.

Singh, R. N. (1997), Neurobiology of the gustatory systems of *Drosophila* and some terrestrial insects, *Microscopy Research and Technique,* 39:547-563.

Spector, A. C. and Travers, S. P. (2005), The representation of taste quality in the mammalian nervous system, *Behavioral and Cognitive Neuroscience Reviews,* 4:143-91.

Stocker, R. F. and Schorderet, M. (1981), Cobalt filling of sensory projections from internal and external mouthparts in *Drosophila*, *Cell and Tissue Research,* 216:513-523.

Stocker, R. F. (1994), The organization of the chemosensory system in *Drosophila melanogaster* - a review, *Cell and Tissue Research,* 275:3-26.

Strausfeld, N. (1970), Golgi studies on insects 2. Optic lobes of Diptera, *Philosophical Transactions of the Royal Society of London Series B-Biological Sciences,* 258:135-223.

Thompson, J. N. and Pellmyr, O. (1991), Evolution of oviposition behavior and host preference in Lepidoptera, *Annual Review of Entomology,* 36:65-89.

Thorne, N., Chromey, C., Bray, S. and Amrein, H. (2004), Taste perception and coding in *Drosophila*, *Current Biology,* 14:1065-1079.

Tingle, F. C. and Mitchell, E. R. (1992), Attraction of *Heliothis virescens* (F) (Lepidoptera, Noctuidae) to volatiles from extracts of cotton flowers, *Journal of Chemical Ecology,* 18:907-914.

van Loon, J. J. A. (1996), Chemosensory basis of feeding and oviposition behaviour in herbivorous insects: a glance at the periphery, *Entomologia Experimentalis Et Applicata,* 80:7-13.

Wang, Z., Singhvi, A., Kong, P. and Scott, K. (2004), Taste representations in the *Drosophila* brain, *Cell,* 117:981-91.

Weiss, L. A., Dahanukar, A., Kwon, J. Y., Banerjee, D. and Carlson, J. R. (2011), The molecular and cellular basis of bitter taste in *Drosophila*, *Neuron,* 69:258-272.

Wessnitzer, J. and Webb, B. (2006), Multimodal sensory integration in insects-towards insect brain control architectures, *Bioinspiration & biomimetics,* 1:63-75.

Windhorst, U. and Johansson, H. (1999). *Modern techniques in neuroscience research,* 1st ed., Springer, Heidelberg, 1325 pp

Wolbarsht, M. L. and Dethier, V. G. (1958), Electrical activity in the chemoreceptors of the blowfly. 1. Responses to chemical and mechanical stimulation, *Journal of General Physiology,* 42:393-412.

Yarmolinsky, D. A., Zuker, C. S. and Ryba, N. J. (2009), Common sense about taste: from mammals to insects, *Cell,* 139:234-44.

Zacharuk, R. Y. (1980), Ultrastructure and function of insect chemosensilla, *Annual Review of Entomology,* 25:27-47.

Zacharuk, R. Y. and Shields, V. D. (1991), Sensilla of immature insects, *Annual Review of Entomology,* 36:331-354.

Zhao, X. C. and Berg, B. G. (2009), Morphological and physiological characteristics of the serotonin-immunoreactive neuron in the antennal lobe of the male oriental tobacco budworm, *Helicoverpa assulta*, *Chemical Senses,* 34:363-372.

8 Appendices

8.1 Appendix I

The “difference” and “colormap” matlab codes generate the net frequency color spectra. The ”difference” code performs the Fourier transformation and creates a net difference between the frequency spectra of the response and spontaneous activity. Furthermore, it rescales the spectra relative to average spontaneous activity (between 20-300 Hz). The ”colormap” code is responsible for importing the spontaneous activity and the response, and for generating labels to the spectrum.

Difference.m

```
function result = difference(x1,x2)
 % Adjust the signal relative to the baseline
 x1 = x1-mean(x1);
 x2 = x2-mean(x2);

 % Make sure the vectors have the same lengths
 if (length(x1) > length(x2))
    x1 = x1(1:length(x2));
 else
    x2 = x2(1:length(x1));
 end

 % Do the Fast Fourier Fourier transformation
 Fs          = 41666;
 nfft        = 2^(nextpow2(length(x1)));
 NumUniquePts = ceil((nfft+1)/2);

 fftx1 = fft(x1,nfft);
 fftx2 = fft(x2,nfft);

 fftx1 = fftx1(1:NumUniquePts);
 fftx2 = fftx2(1:NumUniquePts);

 mx1 = (abs(fftx1)/length(x1)).^2;
 mx2 = (abs(fftx2)/length(x2)).^2;

 if rem(nfft, 2)
    mx1(2:end) = mx1(2:end)*2;
    mx2(2:end) = mx2(2:end)*2;
 else
    mx1(2:end -1) = mx1(2:end -1)*2;
    mx2(2:end -1) = mx2(2:end -1)*2;
 end

 f = (0:NumUniquePts-1)*Fs/nfft;

 % Find the differential spectrum
 diff = mx2 - mx1;

% Convert to only the integral frequencies 0-300 Hz
 original = zeros(1,300);
 result   = zeros(1,300);
```

```
 for i=2:length(diff)
      if (f(i) > 299.9)
         break;
      else
         original(ceil(f(i))) = original(ceil(f(i))) + mx1(i);
         result(ceil(f(i)))   = result(ceil(f(i)))   + diff(i);
      end
   end

   % Rescale result by average spontaneous activity in 20-300 Hz
   result = result ./ (20*sum(original(20:300))/(300-20+1));

   % Remove artifacts due to power grid resonance
   c(1:5) = [0 0 0 0 0];
   result(49)  = c(1); result(50)  = c(1); result(51)  = c(1);
   result(99)  = c(2); result(100) = c(2); result(101) = c(2);
   result(149) = c(3); result(150) = c(3); result(151) = c(3);
   result(199) = c(4); result(200) = c(4); result(201) = c(4);
   result(249) = c(5); result(250) = c(5); result(251) = c(5);
   result(300) = 0;

   % Make sure the result is nice
   smooth(result,5,'loess');
end
```

Colormap.m

```
function colorplot(neuron)
   % Acquire and process input data
   n = size(neuron,2);
   A = zeros(n,300);
   for i=1:n
         [file,path] = uigetfile('*.wav',sprintf('Spontanaktivitet for %s',neuron{i}));
         [x1,f1] = wavread([path,file]);

         [file,path] = uigetfile('*.wav',sprintf('Respons for %s',neuron{i}));
         [x2,f2] = wavread([path,file]);

         A(i,:) = difference(x1,x2);
   end

   % Generate the colorplot itself
   figure('Color',[1 1 1]);
   hold on;
   colormap(makeColorMap([0,0,1],[1,1,1],[1,0,0],256));
   image(A,'CDataMapping','Scaled');
   colorbar('YTickLabel',{'-20','','','','  0','','','','','+20'});
   caxis([-1 1]);
   axis([0 300 0.5 (n+0.5)]);
   set(gca,'YTick',1:n);
   set(gca,'YTickLabel',neuron)

   % Generate separator lines between neurons
   for i=1:n-1
      plot([0,300],[i+0.5,i+0.5],'color','black');
   end
   % Miscellaneous plotting settings
   xlabel('Frequency (Hz)');
   hold off;
end
```

8.2 Appendix II

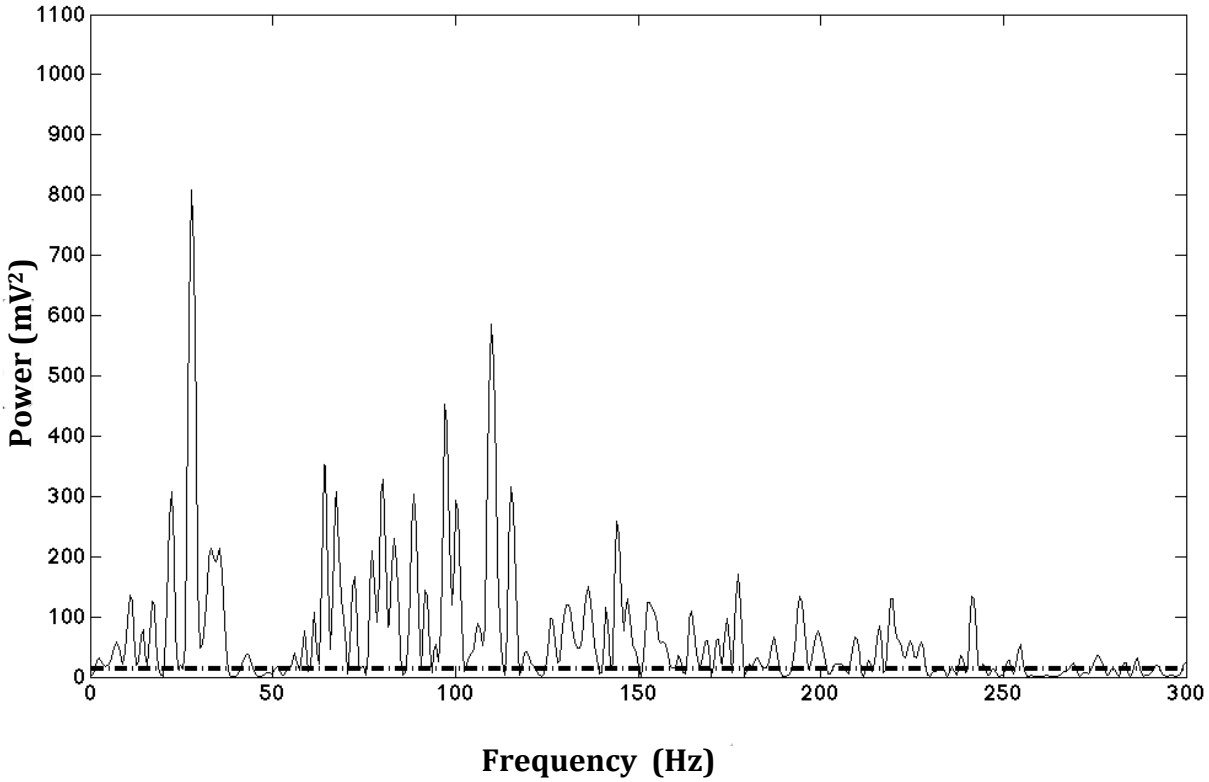

Figure 15. Lomb-Scargle frequency spectrum of the spontaneous activity of GN 26.

8.3 Appendix III

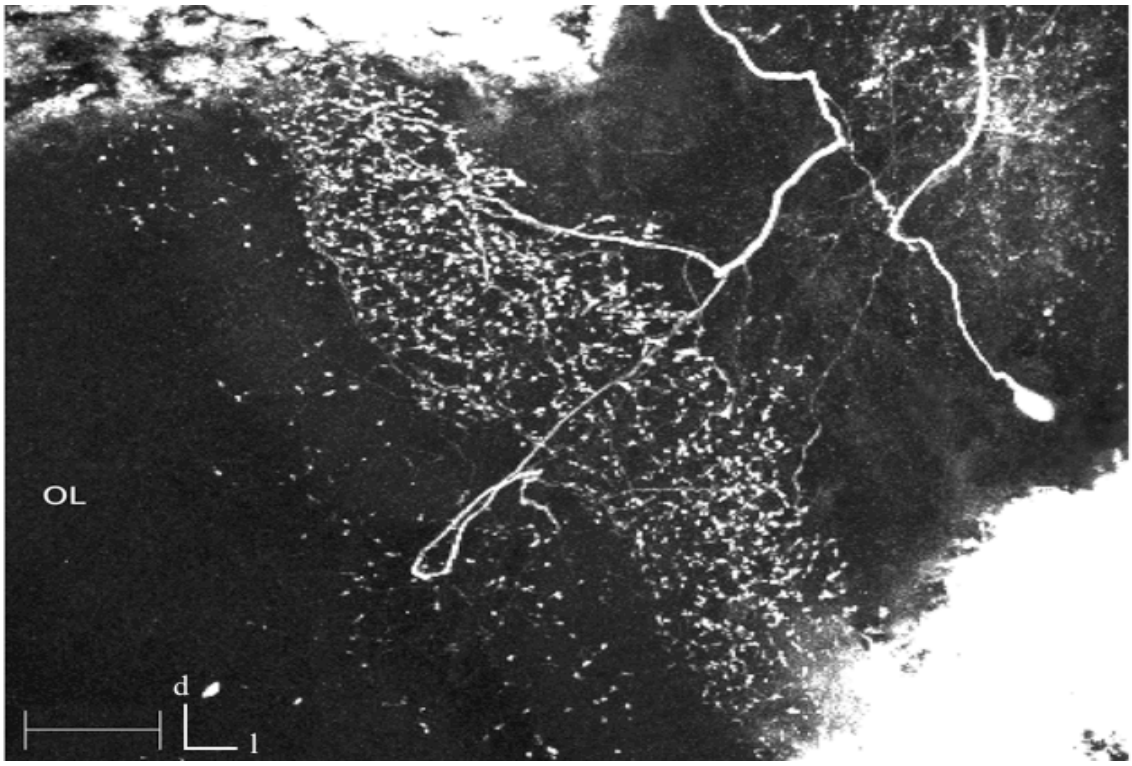

Figure 16. Confocal image of GN 6 in the frontal plane, innervating the lobula complex of the optic lobes. Scale bar = 50 µm.

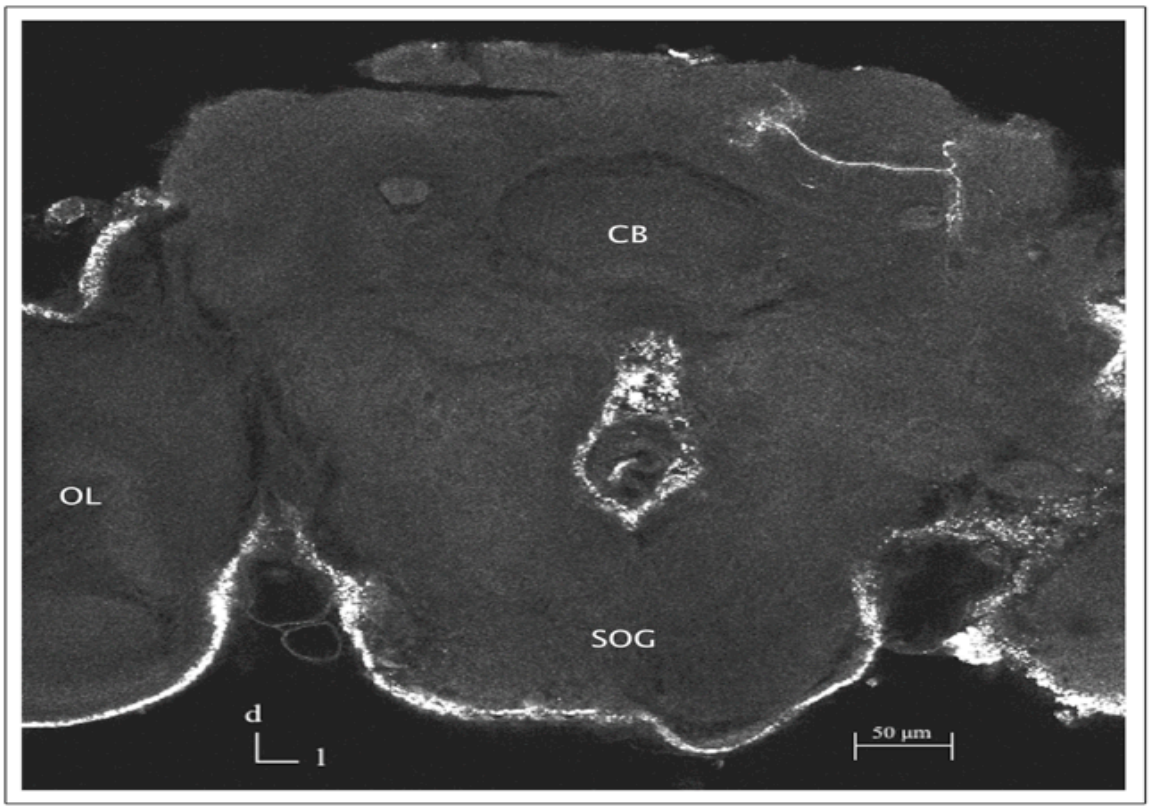

Figure 17. Confocal image of GN 9, showing projections in the dorsolateral to dorsomedial area of the left protocerebrum.

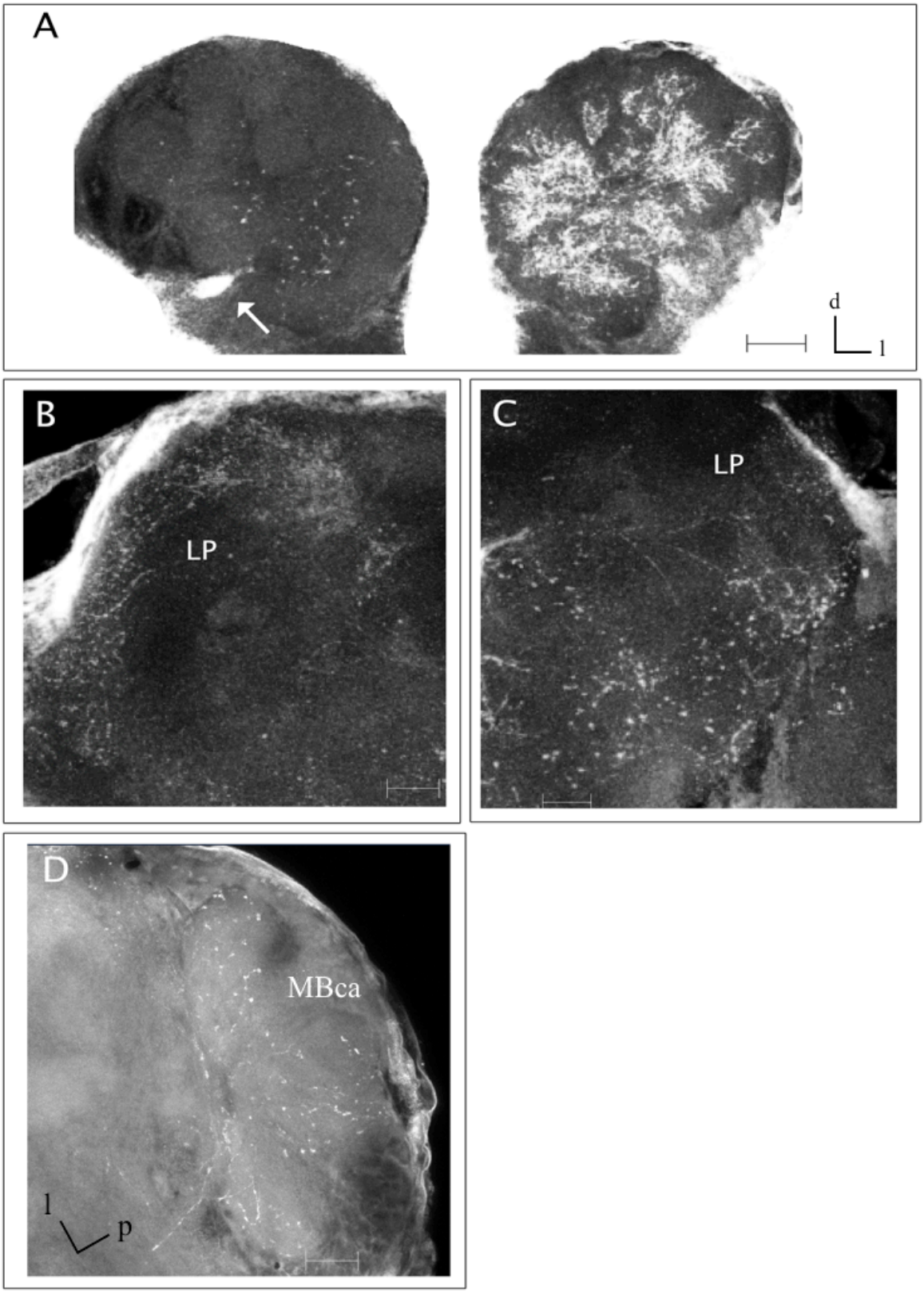

Figure 18. Confocal images of GN 19. (A) Innervation of the left and right antennal lobes. The arrow indicates the soma. (B) and (C) Innervation of the right and left lateral protocerebrum (LP), respectively. (D) Innervation of the left mushroom body calyces (MBca). (A), (B), (C) are in frontal view, (D) is in dorsal view. Scale bar = 50 μm.

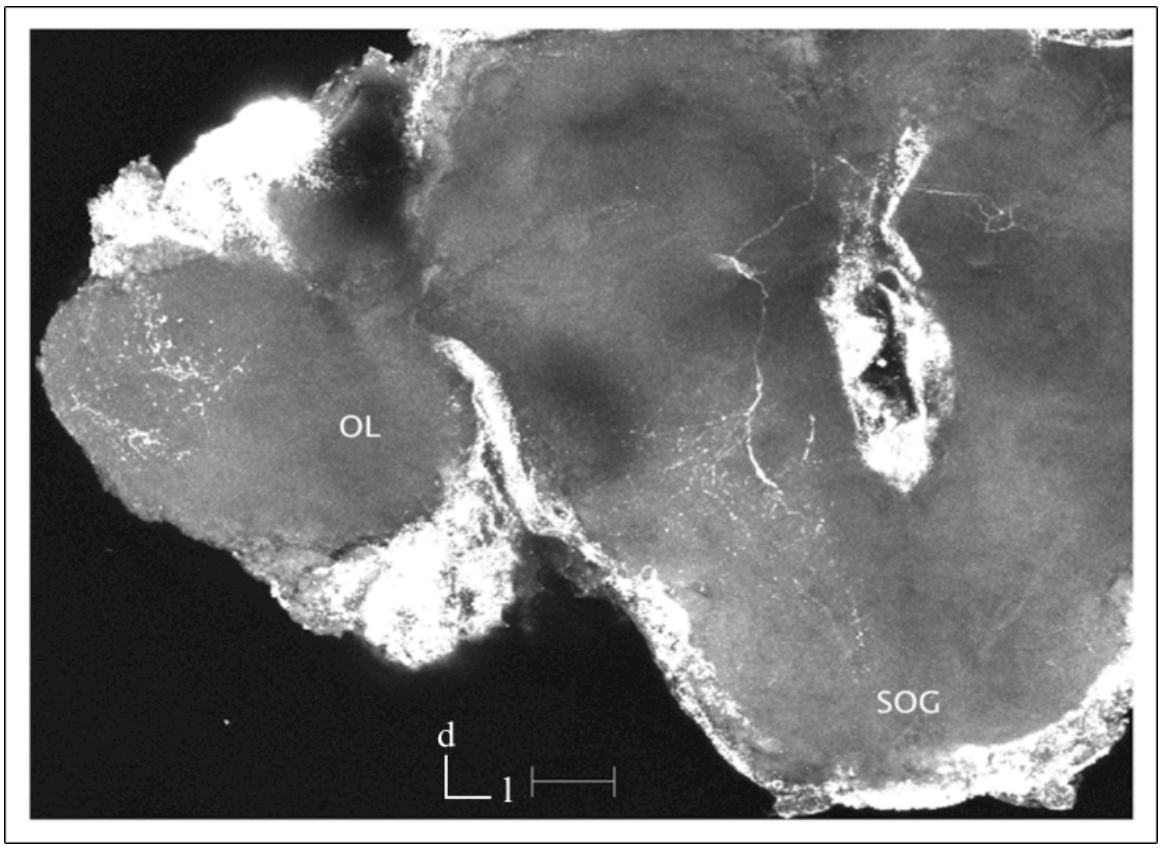

Figure 19. Confocal image of GN 22 in frontal plane, showing innervation of the optic lobes and the tritocerebrum/SOG. Scale bar = 50 µm.

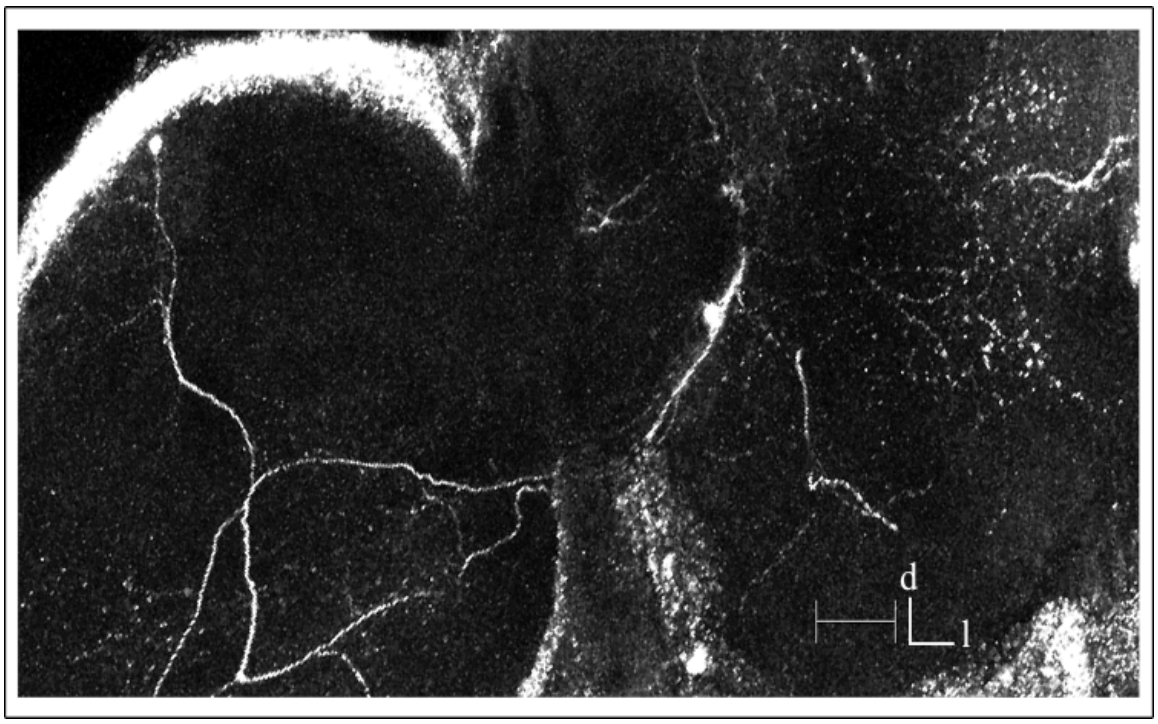

Figure 20. Confocal image of GN 26 in the frontal plane, showing innervation of both the left and right protocerebrum. Scale bar = 50 µm.